Paleoceanography and Paleoclimatology

RESEARCH ARTICLE
10.1029/2020PA004169

Key Points:

- Chironomid head capsules and aquatic leaf waxes from the same sediment samples reflect different lake water isotope seasonality
- Lake water and energy model sensitivity tests compared to proxy records suggest precipitation isotopes and amount changed in the Holocene
- Increased middle Holocene precipitation amount on western Greenland likely caused by greater evaporation from warmer ice-free oceans

Supporting Information:

Supporting Information may be found in the online version of this article.

Correspondence to:

M. C. Corcoran,
megcorcor@gmail.com

Citation:

Corcoran, M. C., Thomas, E. K., & Morrill, C. (2021). Using a paired chironomid δ^{18}o and aquatic leaf wax δ^{2}h approach to reconstruct seasonality on western Greenland during the Holocene. *Paleoceanography and Paleoclimatology*, *36*, e2020PA004169. https://doi.org/10.1029/2020PA004169

Received 17 NOV 2020
Accepted 2 MAR 2021

Using a Paired Chironomid $\delta^{18}O$ and Aquatic Leaf Wax $\delta^{2}H$ Approach to Reconstruct Seasonality on Western Greenland During the Holocene

Megan C. Corcoran[1,2], Elizabeth K. Thomas[1], and Carrie Morrill[3]

[1]Department of Geology, University at Buffalo, Buffalo, NY, USA, [2]Department of Geology, University of Cincinnati, Cincinnati, OH, USA, [3]National Centers for Environmental Information (NCEI), Cooperative Institute for Research in Environmental Sciences (CIRES) University of Colorado at Boulder, Boulder, CO, USA

Abstract The Arctic hydrological cycle is predicted to intensify as the Arctic warms, due to increased poleward moisture transport during summer and increased evaporation from seas once ice-covered during winter. Records of past Arctic precipitation seasonality are important because they provide a context for these ongoing changes. In some Arctic lakes, stable isotopes of oxygen and hydrogen ($\delta^{18}O$ and $\delta^{2}H$, respectively) vary seasonally, due to seasonal changes in precipitation $\delta^{18}O$ and $\delta^{2}H$. We reconstruct precipitation seasonality from Lake N3, a well-dated lake sediment archive in Disko Bugt, western Greenland, by generating Holocene records of two proxies that are produced at different times of the year, and therefore record different lake water seasonal isotopic compositions. Aquatic plants synthesize waxes throughout the summer, and their $\delta^{2}H$ reflects winter-biased precipitation $\delta^{2}H$ at Lake N3, whereas chironomids synthesize their head capsules between late summer and winter, and their $\delta^{18}O$ reflects summer-biased precipitation $\delta^{18}O$ at Lake N3. During the middle Holocene at Lake N3, aquatic plant leaf wax was strongly ^{2}H-depleted, while chironomid chitin was ^{18}O-enriched. We guide interpretations of these records using sensitivity tests of a lake water and energy balance model, where we change precipitation amount and isotope seasonality inputs. The sensitivity tests suggest that the contrasting trends between proxies were likely caused by an increase in precipitation amount during all seasons and an increase in precipitation isotope seasonality, in addition to proxy-specific mechanisms, highlighting the importance of understanding lake- and proxy-specific systematics when interpreting records from sediment archives.

1. Introduction

The Arctic hydrological cycle is predicted to intensify as climate warms due to increased poleward moisture transport and greater evaporation in areas previously covered by sea ice (Bintanja & Selten, 2014; Kopec et al., 2016). These mechanisms have different seasonal expressions: reduction of sea ice during fall and winter months causes an increase in local evaporation and thus more fall and winter precipitation, whereas strengthening of the meridional moisture gradient due to increasing temperature causes an increase mainly in summer precipitation (Bintanja & Selten, 2014). Changes in Arctic precipitation seasonality may influence feedbacks between hydroclimate, atmospheric and ocean circulation, and plant communities, and are important for projections of sea level rise and ice sheet dynamics (Bintanja & Selten, 2014; McMillan et al., 2016; Nerem et al., 2018; Post et al., 2009).

Records of precipitation seasonality, amount, and isotopic composition during past warm times, such as the middle Holocene, may provide context for the response of the hydrological cycle to ongoing climate changes (Kaufman et al., 2004; Masson-Delmotte et al., 2005; Thomas et al., 2016). Yet, Holocene records of these variables in the Arctic are limited. Ice core isotope records are often continuous through the Holocene, but seasonality is hard to capture due to small amounts of snow accumulation and increased compaction deeper in the core (Cuffey & Clow, 1997; Cuffey & Steig, 1998). Many lakes are affected by evaporation, which overprints the precipitation isotope signal (N. J. Anderson & Leng, 2004; Balascio et al., 2013; Jepsen et al., 2013; Krabill et al., 2004; Schiff et al., 2009). There are a limited number of records from Arctic lakes that reflect precipitation isotopes (L. Anderson et al., 2001; Balascio et al., 2018; Lasher et al., 2020; Thomas et al., 2018, 2020). Developing proxy records in lakes that can be used to reconstruct precipitation isotopes

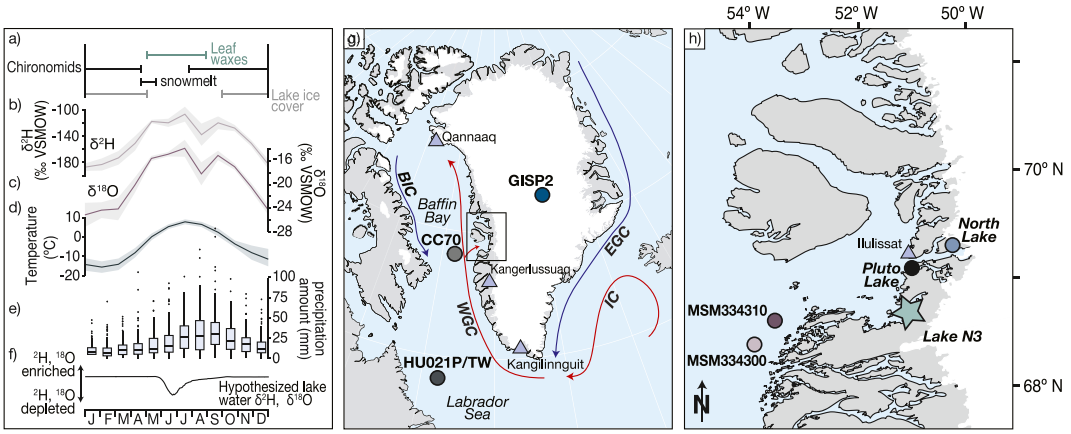

Figure 1. Map of study site and modern climatology in Disko Bugt region, western Greenland. (a) Schematic showing timing of snowmelt and ice cover and synthesis of chironomid head capsules and aquatic plant leaf waxes based on observations ((Butler, 1982; Guo et al., 2013; Lindegaard & Mæhl, 1992). (b) Monthly precipitation δ^2H and (c) $\delta^{18}O$ at Lake N3 (OIPC, version 3.1) (Bowen, 2020; Bowen et al., 2003; IAEA/WMO, 2020). (d) Temperature (n = 140 years, 1880–2020) and (e) precipitation amount n = 112 years, 1880–1992) at Ilulissat (1880–1960: 69.2167° N, 51.05° S, 1961–1992: 69.22 °N, 51.1° S, 1992–2020: 69.2331° N, 51.0667° S) (NOAA, 2020). Shading in b, c and d shows 1 standard deviation from the mean (solid lines). Boxes in e are quartiles about the median, whiskers are 5 and 95 percentiles, and dots are outliers. (f) Hypothesized lake water isotopes throughout the year, based on precipitation isotopes, and the timing of lake ice cover and snowmelt. (g) Greenland and surrounding regions showing locations of meteorological and precipitation isotope data, Qanaaq, Kangerlussuaq and Kangilinnguit (triangles) (IAEA/WMO, 2020), GISP2 ice core (blue dot), ocean sediment cores, CC70 (gray dot) and HU84-030-012TWC/PC (HU021P/TW), (black dot) (de Vernal et al., 2013; Gibb et al., 2015). Arrows indicate currents, East Greenland Current (EGC), West Greenland Current (WGC), Baffin Island Current (BIC), Irminger Current (IC). Red and blue are warm and cool currents, respectively. (h) Disko Bugt region, western Greenland showing Ilulissat (triangle), Lake N3 (green star) (Thomas et al., 2016), Pluto Lake (black dot), North Lake (blue dot) (Axford et al., 2013), and ocean sediment cores MSM334310 and MSM334300 (dark and light purple circles, respectively) (Ouellet-Bernier et al., 2014).

and seasonality is essential to understanding future changes in the hydrological cycle (Corcoran et al., 2020; Thomas et al., 2020).

The stable isotopes of oxygen and hydrogen ($\delta^{18}O$ and δ^2H, respectively) in precipitation vary seasonally in much of the Arctic, due to seasonal changes in moisture source, temperature, transport history, and phase (Bowen et al., 2019; Dansgaard, 1964). For example, at our study site on western Greenland, Lake N3, based on modeled precipitation isotopes estimated from the online isotopes in precipitation calculator (OIPC) v. 3.1, winter (October to February) precipitation is about 45‰ ^2H- and 7‰ ^{18}O-depleted compared to summer (June to September) precipitation (Figures 1b and 1c) (Bowen, 2020; Bowen & Revenaugh, 2003; Cluett & Thomas, 2020; IAEA/WMO, 2020). Where this strong seasonal precipitation isotope signal is present and preserved in proxies found in lake sediment archives, it may be used to reconstruct changes in precipitation seasonality (Nichols et al., 2009; Thomas et al., 2020).

Lake water isotopic composition reflects the isotopic composition of the precipitation that falls on the surrounding catchment area and into the lake. The lake water isotopic composition is also determined by the water residence time of the lake (Gibson et al., 2016; Jonsson et al., 2009). If the lake water residence time is short, meaning the lake is flushed rapidly, then the isotopic composition of the lake water will change seasonally, in step with changes in precipitation isotopic composition (Jonsson et al., 2009; Thomas et al., 2020). An increase in precipitation amount would result in a shorter residence time, causing the lake water isotopic composition to change more dramatically on a seasonal basis. Moreover, a faster residence time would mean less opportunity for evaporative enrichment, and less of the evaporated signal would be preserved from one year to the next (Cluett & Thomas, 2020). During winter, when Arctic lakes are covered by ice, the lake water isotopic composition remains constant and reflects late summer precipitation isotopic composition (Figures 1b, 1c, and 1f) (Gibson, 2002; Jonsson et al., 2009; Saulnier-Talbot et al., 2007). During a brief (1 week–1 month) period in spring, snow and ice melt, flushing large volumes of ^2H- and ^{18}O-depleted winter precipitation from the lake catchment through the lake (Jonsson et al., 2009; Thomas et al., 2020;

Tondu et al., 2013). Variations in lake water isotope values throughout the year allow lake water proxies to capture different lake water seasonality, if the proxies themselves are formed at different times of the year.

Oxygen or hydrogen isotopes ($\delta^{18}O$, $\delta^{2}H$) of proxies preserved in lake sediment archives reflect the source water, in this case lake water, in which they are synthesized (Corcoran et al., 2020; Sachse et al., 2012; van Hardenbroek et al., 2018). These proxies reflect a specific lake water seasonality, depending on the timing of synthesis (Castañeda & Schouten, 2011). Here, we use aquatic leaf wax (C_{24} *n*-alkanoic acid) $\delta^{2}H$ ($\delta^{2}H_{wax}$) and chironomid head capsule (mostly chitin) $\delta^{18}O$ ($\delta^{18}O_{chir}$) as proxies of lake water $\delta^{2}H$ ($\delta^{2}H_{lw}$) and $\delta^{18}O$ ($\delta^{18}O_{lw}$). These two proxies have distinct and different seasons of production, and therefore have potential to reflect different lake water isotope seasonality (Butler, 1982; Guo et al., 2013; Lindegaard & Mæhl, 1992).

Leaf waxes are long-chained organic compounds produced by plants as a protective coating (Tipple et al., 2013). Aquatic plants, typically dominated by aquatic mosses in the Arctic, produce their biomass (stems and leaves) throughout the ice-free growing season (May to September at Lake N3) (Guo et al., 2013; Riis et al., 2014). Aquatic plants therefore incorporate lake water hydrogen into leaf waxes mainly during the growing season (Figures 1a and 1f). Leaf wax proxy systematics at Lake N3 are discussed in detail elsewhere (Thomas et al., 2016, 2020), but in summary, sedimentary *n*-alkanoic acid distributions are similar to those in modern aquatic mosses, and $\delta^{2}H$ of the C_{24} *n*-alkanoic acid has very different Holocene values and trends than the C_{26} and C_{28} *n*-alkanoic acid. We therefore interpret the C_{24} *n*-alkanoic acid to be derived mainly from aquatic mosses in the Lake N3 record (Thomas et al., 2016, 2020). At Lake N3, aquatic plant leaf waxes incorporate lake water that contains ^{2}H-depleted winter snowmelt in addition to summer precipitation (Figures 1a and 1f), so we interpret C_{24} $\delta^{2}H$ as winter-biased mean annual precipitation $\delta^{2}H$.

Chironomids are non-biting aquatic midges (Insecta: Diptera: Chironomidae) whose larval head capsules are mostly made of chitin. The $\delta^{18}O$ value of the head capsules reflects both the $\delta^{18}O_{lw}$ in which the larvae grew (~70% of the isotope signal) and the diet of the larvae (~30% of the isotope signal) (Wang et al., 2009). Arctic chironomids have a multi-year life cycle lasting up to seven years, during which they develop through four instars. When larvae grow to the next instar, their head capsules are shed and preserved in lake sediment archives for thousands of years (Butler, 1982; Hershey, 1985; van Hardenbroek et al., 2018). The transition in Arctic chironomids from the third to fourth instar, or the time when the fourth instar chitinous head capsules form, occurs sometime between late July and the following winter, prior to spring snowmelt (Butler, 1982; Butler & Braegelman, 2018; Lindegaard & Mæhl, 1992; Valero-Garcés et al., 1997). The $\delta^{18}O$ of the head capsule of the fourth instar, which is the stage that we sample for this study, therefore reflects late summer and winter $\delta^{18}O_{lw}$. Because Lake N3 is nearly completely flushed with summer precipitation by July and water in ice-covered Arctic lakes remains at late summer precipitation isotope values throughout the ice-cover season, we interpret $\delta^{18}O_{chir}$ in Lake N3 to reflect summer-biased mean annual precipitation $\delta^{18}O$ (Figures 1a–1c and 1f). The lake water today is impacted by evaporative enrichment, the isotopic fingerprint of which is preserved from one year to the next, influencing both the leaf wax and chironomid isotope proxies (details in Section 2.1).

Previous studies at Lake N3 have inferred relative changes in winter precipitation amount and isotopic composition during the Holocene using $\delta^{2}H$ of aquatic and terrestrial plant leaf waxes (Thomas et al., 2016, 2020). The Lake N3 aquatic plant $\delta^{2}H_{wax}$ record shows a nearly 100‰ ^{2}H-depletion from 6 to 4 ka relative to the late Holocene which may have been due to several mechanisms such as a relative increase in winter precipitation amount, ^{2}H-depleted precipitation, and a decrease in the amount of snowmelt bypass (i.e., less snow melts off the landscape before the lake becomes ice free, so more snow melt water enters the lake basin during the spring freshet) (Thomas et al., 2016, 2020). The $\delta^{2}H$ of long-chain *n*-alkanoic acids (C_{28}), produced by terrestrial plants in the Lake N3 catchment, reflects summer precipitation $\delta^{2}H$, but is also affected by evaporative ^{2}H-enrichment of leaf water (Rach et al., 2017; Sachse et al., 2006). Seasonal precipitation amount or isotopic composition therefore cannot be inferred from the combination of terrestrial and aquatic plant $\delta^{2}H_{wax}$ alone. Complementing the aquatic plant $\delta^{2}H_{wax}$ record with another lake water isotope proxy that captures a different season would provide insights into how lake water cycled in the Holocene and how precipitation seasonality, amount, and isotopes changed during the middle Holocene.

Here, we test the hypothesis that paired $\delta^{18}O_{chir}$ and aquatic plant $\delta^{2}H_{wax}$ records from Lake N3 on western Greenland contain different Holocene values and trends because they reflect different isotope seasonality.

We perform sensitivity tests with the Environment sub-model of PRYSM 2.0, a lake proxy system forward model, to qualitatively assess the precipitation amount and isotopic composition needed to cause the water isotope trends observed in the $\delta^{18}O_{chir}$ and aquatic plant $\delta^{2}H_{wax}$ records (Dee et al., 2015, 2018; Hostetler & Bartlein, 1990, 1994). We use the two isotope records from this one site to infer millennial-scale changes in precipitation seasonality and relative changes in precipitation amount during the Holocene.

2. Methods and Approach

2.1. Study Site

Lake N3 is a small through-flowing lake located on the Nuuk Peninsula in southeastern Disko Bugt, western Greenland (Figures 1g and 1h). At Lake N3, precipitation amount and temperature are highest during summer and early fall (Figures 1d and 1e) (NOAA, 2020). Lake N3 is ice-free from May to September. The sediments in the Lake N3 core are composed of primarily gyttja over the past 8.0 ka. Sand deposited before 8.0 ka and Greenland Ice Sheet moraines that lie east of Lake N3 catchment indicate that the lake received ice sheet meltwater prior to, but not after, 8.0 ka (Briner et al., 2010; Thomas et al., 2016; N. E. Young et al., 2013). There are no evaporites or other coarse layers in the lake N3 sediment cores, indicating that the lake was never extremely evapoconcentrated, nor experienced dramatically lower lake levels during the past 8,000 years (Thomas et al., 2016). Seasonal Lake N3 water residence time (i.e., the mean time that a molecule of water stays in the lake) was recalculated in Thomas et al. (2020). Under modern conditions, Lake N3 has a 'spring melt' residence time of 5 months. According to a simple box model (Thomas et al., 2020), the isotopic composition of the lake water becomes depleted in heavy isotopes during the spring melt, resulting in lake water isotope values to reflect winter-biased mean annual precipitation isotope values during early summer. Subsequently in summer, precipitation flushes through Lake N3 via several inflow streams, where slower flow of water through the lake means a water residence time of 24 months. As the relatively ^{18}O- and ^{2}H-enriched summer precipitation flows through the lake, the lake water becomes enriched in the heavy isotopes. In addition, the lake is subject to some evaporative enrichment during the summer. Modern surface lake water collected on July 27, 2010 has a $\delta^{2}H$ and $\delta^{18}O$ of −96.1‰ and −11.3‰, respectively (Table S4), and d-excess is −5.3‰, indicating around 10%–20% of the lake water is lost to evaporation (Cluett & Thomas, 2020). If the lake water is not completely flushed each year, the evaporation signal may be preserved from one year to the next (Jonsson et al., 2009). As climate changes with increases in precipitation amount, lake water isotopic composition may become more inflow-sensitive (Cluett & Thomas, 2020). In general, we interpret water isotopes in Lake N3 as reflecting seasonal variations in regional precipitation isotopes with some evaporative enrichment, meaning that proxies for lake water isotopes may reflect past changes in precipitation seasonality.

Sediment core collection and storage was described previously (Thomas et al., 2016). The age model for Lake N3 core 10N3-2A was generated using eight radiocarbon-dated aquatic macrofossils (Thomas et al., 2016). Leaf wax records of all carbon chain lengths (C_{24}–C_{28}) were published in Thomas et al. (2016) and are discussed in detail in Thomas et al. (2020). Depth profiles of temperature, conductivity, salinity, pH and dissolved oxygen from two separate locations in Lake N3 were also measured at the time of core collection on July 27, 2010 (see Figures S4 and S5 and Tables S2 and S3).

2.2. Chironomid Sample Preparation

Between 0.32 and 1.41 g of sediment were sampled from core 10N3-2A at the same depths as 20 of the samples analyzed for leaf waxes. Sediment was taken from a 0.5-centimeter-thick section of the core, with additional sediment added from neighboring depths if there were not enough chironomids for isotope analysis. Samples were prepared for chironomid isotope analysis following previously published methods (Arppe et al., 2017; Lasher et al., 2017; Verbruggen et al., 2010; Wang et al., 2008). Dry sediment was deflocculated in a 10% KOH bath at room temperature for 30 min, stirring halfway through. Sediment was rinsed with DI water over a 100 μm sieve. Chironomid head capsules in each sample were hand-picked at 4x to 40x magnification, isolated, and counted. Head capsules were recounted for accuracy and to confirm that they were free of sediment prior to being transferred to pre-massed 5 by 3.5 mm lightweight Elemental Microanalysis silver capsules. Two hundred to 790 independent head capsules were isolated per sample. Samples were

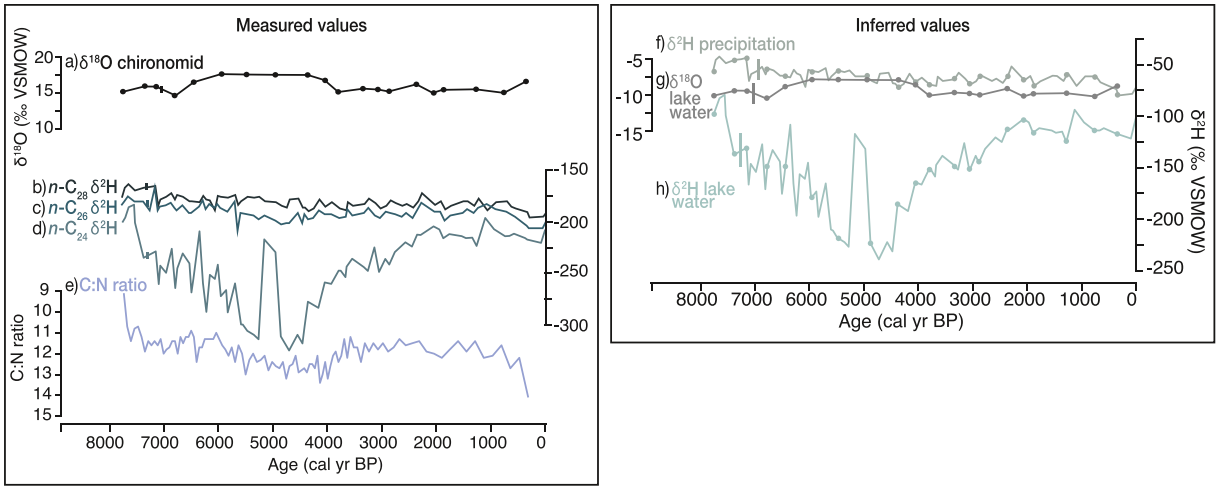

Figure 2. Measured and inferred Holocene records of $\delta^{18}O_{chir}$ and aquatic plant $\delta^{2}H_{wax}$ and lake water $\delta^{18}O$ and $\delta^{2}H$ from Lake N3. (a) $\delta^{18}O_{chir}$ record (black). (b-d) Leaf wax $\delta^{2}H$ of C_{28}, C_{26}, and C_{24} respectively (Thomas et al., 2016). (e) (c:N ratio from Lake N3. (f) Calculated spring and summer precipitation $\delta^{2}H$ (McFarlin et al., 2019; Thomas et al., 2016). (g) Calculated fall and winter lake water $\delta^{18}O$ (gray) (Lasher et al., 2017). (h) Calculated spring and summer lake water $\delta^{2}H$. Dots in f and h correspond to the samples where chironomids were picked and analyzed. Vertical lines on (a) through (d) and (f) through (h) are average uncertainties for all data points in the record, including analytical and fractionation factor uncertainties.

slightly crimped in these silver capsules and freeze dried for 5 days before being completely crimped and massed (Bowen et al., 2005). Hot acid or base baths were not used as they may remove chitin and alter the $\delta^{18}O$ composition of the head capsules (Verbruggen et al., 2010; Wang et al., 2008).

2.3. Chironomid Chitin $\delta^{18}O$ Analysis

Chironomid chitin $\delta^{18}O$ was analyzed on a thermal conversion elemental analyzer coupled to an isotope ratio mass spectrometer at the UC Davis Stable Isotope Facility. Nylon and Alanine were used as lab references for order correction, size correction and elemental totals. Results were normalized to VSMOW using IAEA-600 and USGS-35 international isotopic reference standards. Cellulose (31.2‰ $\delta^{18}O$) and chitin (28.0‰ $\delta^{18}O$) were used for internal checks during analysis. Analytical uncertainty of these measurements was 0.4‰.

2.4. Conversion to Source Water $\delta^{2}H$ and $\delta^{18}O$

In order to directly compare the two isotope proxy records, $\delta^{18}O_{chir}$ and aquatic $\delta^{2}H_{wax}$, were converted to $\delta^{18}O_{lw}$ and $\delta^{2}H_{lw}$ (Figures 2a, 2d, 2g, and 2h). These conversions were made using published biological fractionation factors for $\delta^{18}O_{chir}$, $\varepsilon = 22.4 \pm 1.3$‰ (Lasher et al., 2017; van Hardenbroek et al., 2018; Verbruggen et al., 2011) and for aquatic C_{24} $\delta^{2}H_{wax}$, $\varepsilon = -112 \pm 33$‰ (McFarlin et al., 2019). Lake water $\delta^{18}O$ was calculated using the following equation (Equation 1):

$$\varepsilon_{chir/lw} = \left(\frac{\left(1{,}000 + \delta^{18}O_{chir}\right)}{\left(1{,}000 + \delta^{18}O_{lw}\right)} \right) - 1 \quad (1)$$

$\delta^{2}H_{lw}$ was calculated using the same equation but with the respective $\delta^{2}H_{wax}$ values. We discuss assumptions and limitations of these fractionation factors in Section 4.2.2.

In order to directly compare lake water isotope values inferred from chironomids and aquatic plant leaf waxes, we convert chironomid-inferred $\delta^{18}O_{lw}$ values to the $\delta^{2}H$ scale using the local meteoric water line from Lake N3, western Greenland ($\delta^{2}H = 6.8 * \delta^{18}O - 13.7$) estimated from the OIPC v. 3.1 (Bowen, 2020; Bowen & Revenaugh, 2003; IAEA/WMO, 2020). This conversion was also completed using local meteoric water lines established using monthly precipitation isotope data at Qaanaaq (76.52 °N, 68.83 °W), ($\delta^{2}H = 7.3$

* $\delta^{18}O + 7.2$; $n = 5$ years, monthly-based measurements) and Kangilinnguit (61.22°N, 48.12°W), ($\delta^{2}H = 6.6 * \delta^{18}O - 19.2$; $n = 8$ years), which yielded values within uncertainty of the values determined using the Lake N3 meteoric water line (IAEA/WMO, 2020).

Terrestrial leaf wax (C_{28} *n*-alkanoic acid) $\delta^{2}H$ was converted to precipitation $\delta^{2}H$ to facilitate comparison with the Holocene lake water isotope values (Figure 2b). This conversion was made using the published global compilation fractionation factor between C_{28} *n*-alkanoic acids extracted from lake surface sediments and precipitation, $\varepsilon = -99 \pm 32‰$ and using the above equation (McFarlin et al., 2019).

2.5. Environment Sub-model of PRYSM

We ran sensitivity tests with the Environment sub-model of PRYSM 2.0 from Dee et al. (2018), which was originally developed by Hostetler and Bartlein (1990) and Hostetler and Benson (1994), to assess two possible mechanisms, changing precipitation amount and changing precipitation isotopes, that may have caused the fluctuations observed in the Lake N3 Holocene lake water isotope records. Daily meteorological inputs (air temperature, relative humidity, wind speed, surface incident shortwave radiation, downward longwave radiation, surface pressure, and precipitation amount) for this model were acquired from ERA-Interim Global Reanalysis Data set for 1980–2016 (Dee. et al., 2018). Temperature and relative humidity inputs were bias-corrected using quantile mapping with observed measurements from Ilulissat (Morrill et al., 2019; Reiter et al., 2018) (https://github.com/carriemorrill/lake-model-utilities). To simulate water and isotopic balance for the lake, the amount and timing of catchment runoff to the lake and values for $\delta^{2}H$ and $\delta^{18}O$ for precipitation and runoff are additionally needed. Runoff amount was calculated using 20% of the precipitation amount acquired from the ERA-Interim data set, a reasonable estimate for lake catchments in coastal Arctic settings (Gibson et al., 2002; Welp et al., 2005), but a poorly constrained value for individual catchments. In the supplemental materials, we present a sensitivity analysis showing that this assumption yields a simulated modern water balance that is reasonable. Runoff was set to 0 mm/day during the ice cover season, as we assume that all snow remains on the landscape until the spring snowmelt (Jonsson et al., 2009). The snowmelt period was started for each individual year when temperatures were above freezing for more than two consecutive days. The length of the snowmelt period was set to three weeks based on our assumption that Lake N3 is similar to the snowmelt timing in observational studies of other high latitude lakes (see supplement Section S1 for more details) (FitzGibbon & Dunne, 1981; Roulet & Woo, 1988). Total winter snowfall was divided into 21 days to simulate the snowmelt period, with runoff calculated as 20% of the total snow water equivalent, unless otherwise stated. Monthly precipitation $\delta^{2}H$ and $\delta^{18}O$ were determined using the OIPC (Figures 1b and 1c) (Bowen, 2020; Bowen & Revenaugh, 2003; IAEA/WMO, 2020). Amount-weighted $\delta^{2}H$ and $\delta^{18}O$ of runoff were calculated assuming that runoff has the same isotope values as precipitation. Appropriate values for lake model parameters including the shortwave coefficient, fraction of advected air, and neutral drag coefficient were determined for Lake N3 by comparing model output temperature, mixing depth, and surface $\delta^{18}O_{lw}$ and $\delta^{2}H_{lw}$ to the field measurements taken during sample collection on July 27, 2010, see Section S1 in the supplement for more information on selecting model parameters (Figure 3, Table S1) (Dee et al., 2015, 2018). We acknowledge that we only have modern observations from one day to calibrate the model, due to limited access to the remote field site, however, multiple parameter comparisons between our observations and the model builds our confidence in the model performance. Due to these limited observations we qualitatively interpret sensitivity tests to precipitation amount and isotopes run using this version of the model, and look to future work that incorporates year-round lake water monitoring to more robustly calibrate the model.

Once model parameters were set to reproduce the modern observations at Lake N3 on July 27, 2010, input precipitation isotopes and precipitation amount were changed to assess the sensitivity of the lake water isotopic composition to these variables. Ice-free season (June, July, August, September) precipitation isotope values and amount and late fall and winter or the ice-cover season (October, November, December, January, February) precipitation isotope values and amounts were each changed individually to determine their impact on lake water isotope values. Changes in precipitation isotope values were determined using the range of modern precipitation isotope values at Global Network of Isotopes in Precipitation stations north and south of our study site on western Greenland: Qaanaaq and Kangilinnguit (Figure 1g). For these experiments, precipitation isotope values were increased by 20‰ $\delta^{2}H$ (2.5‰ $\delta^{18}O$) during the ice-free season

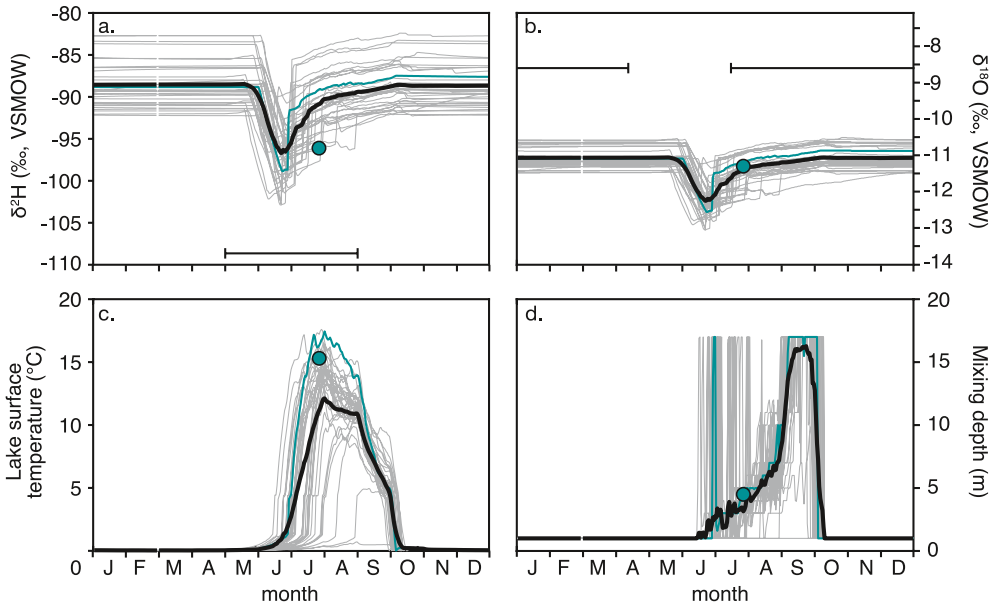

Figure 3. Results from the Environment sub-model of PRYSM (Dee et al., 2018) for Lake N3 run using modern parameters (1980–2016 CE). (a) Surface lake water δ^2H, (b) Surface lake water $\delta^{18}O$, (c) Lake surface water temperature, (d) Mixing depth. Light gray lines: individual years, turquoise line: modeled values using meteorological variables for 2010 CE, black line: mean of all 36 years. Turquoise dot: measurements on July 27, 2010. Black horizontal bar: modern δ^2H_{lw} and $\delta^{18}O_{lw}$ determined from uppermost sediment sample from C_{24} *n*-alkanoic acid δ^2H and chironomid $\delta^{18}O$ records, plotted during the season when the proxy is produced.

to match summer precipitation isotope values at Kangilinnguit and decreased by 50‰ δ^2H (6.4‰ $\delta^{18}O$) during the ice-cover season to match winter precipitation isotope values at Qaanaaq (Figure S1) (IAEA/WMO, 2020). A Holocene aquatic plant δ^2H_{wax} record from, a nearby lake (Pluto Lake) on western Greenland near Ilulissat (Figure 1h), suggests that there was about a 15‰ δ^2H increase in summer precipitation isotopes at about 6 ka in this region (Thomas et al., 2020), which we test here by increasing summer precipitation isotopes by 20‰ in the model. Precipitation deuterium excess values in each of these experiments were kept the same as in the modern scenario.

Paleoclimate records of Arctic precipitation amount are rare, but those that exist suggest that winter precipitation and to some extent summer precipitation amount increased during the middle Holocene (Andreev & Klimanov, 2000; Andresen et al., 2004; Nichols et al., 2009). For our experiments, precipitation amount was increased to 200% of the precipitation falling into the lake in the ice-free season and in the ice-cover season, a value that is likely an overestimate. Runoff amount and isotopes were adjusted in the input file to reflect changes in precipitation isotope values and amounts for each model sensitivity run. Lastly, all four of these variables were changed at the same time to determine how lake water isotopes respond to the combination of changing precipitation isotope values and amount. This combination scenario was run with runoff set at both 20% and 50% of precipitation. The daily values for each of 36 years of model output for each sensitivity test were averaged in order to compare the seasonal trends in lake water isotope values between different scenarios.

3. Results

$\delta^{18}O_{chir}$ ranges from 11.6 ± 0.4‰ to 14.6 ± 0.4‰ throughout the record (Figure 2a). From 6.5 to 4.0 ka, $\delta^{18}O_{chir}$ mean and standard deviation is 14.2 ± 0.5‰, compared to a mean and standard deviation of 12.5 ± 0.5‰ of all other samples. The timing of the transition from ^{18}O-depleted to ^{18}O-enriched chitin in the middle Holocene corresponds to the timing of the transition from ^2H-enriched to ^2H-depleted aquatic plant leaf wax in the same samples. Calculated $\delta^{18}O_{lw}$ values based on $\delta^{18}O_{chir}$ range from −10.6 to −7.6‰ in this record (Figure 2f). Calculated δ^2H_{lw} values based on aquatic plant δ^2H_{wax} range from −239.4‰ to −80.2‰ (Figures 2d and 2h). After converting oxygen isotopes to the hydrogen isotope scale using the local meteoric

water line at Lake N3, the magnitude of the δ^2H_{lw} generated by δ^2H_{wax} change is about six times that of the change observed in the $\delta^{18}O_{lw}$ inferred from the $\delta^{18}O_{chir}$ record, and is in the opposite direction (Figures 2g and 2h). Lake N3 water δ^2H values inferred from $\delta^{18}O_{chir}$ is around 50‰ ^{2}H-enriched compared to Lake N3 water inferred from aquatic plant δ^2H_{wax} during most of the Holocene, but is up to 150‰ ^{2}H-enriched from 4 to 6 ka. Calculated source (precipitation) water δ^2H values for C_{28} terrestrial plant δ^2H_{wax} range from −79.7‰ to −42.2‰ (Figures 2b and 2f).

3.1. PRYSM Environment Sub-model Results

Comparisons between modern lake water variables (mixing depth, surface (0–1 m) temperature, and surface water isotope values) generated using the Environment sub-model of PRYSM and measured lake water conditions from July 27, 2010 were made to constrain the model using multivariate measurements. The modeled modern lake water variables show good agreement with the measured modern lake water variables, indicating that this model can be used to simulate conditions at Lake N3 (Figure 3). Modern lake water measurements of temperature, conductivity, salinity, pH and dissolved oxygen can be found in Figures S4 and S5. Modern δ^2H_{lw} and $\delta^{18}O_{lw}$ on July 27, 2010 was −96.1 ± 1.1‰ and −11.3 ± 0.07‰, respectively (1σ, $n = 3$) (Table S4) (Thomas et al., 2016). Modeled lake water isotope values on July 27, 2010 were −89.2‰ for δ^2H and −11.2‰ for $\delta^{18}O$ (Figures 3a and 3b). Measured surface lake water temperature was 15.5 ± 0.3 °C ($n = 2$). Modeled lake water temperatures range from 11.1°C to 17.4 C with a mean of 14.7 C for July 27th for all 36 years of the modern simulation (Figure 3c). Measured mixing depth determined from the temperature depth profiles of Lake N3 (see Figures S4 and S5) on July 27, 2010 was 4.0–4.5 m ($n = 2$). Modeled mean mixing depth in N3 on July 27, 2010 was 4.0 m, with a mean of 3.15 m for July 27th of all 36 years (Figure 3d). The lake was ice-free during July 2010 fieldwork, a variable also matched by the model. δ^2H_{lw} and $\delta^{18}O_{lw}$ changes throughout the year using the PRYSM model are of smaller magnitude than the precipitation seasonality gradient observed in the modeled precipitation δ^2H and $\delta^{18}O$ over the course of the year (Figure S1) (Bowen, 2020; Bowen & Revenaugh, 2003; IAEA/WMO, 2020). The model appears to be slightly biased in δ^2H_{lw} values, with values too high in the model relative to observations. Changing model parameters were unable to match δ^2H_{lw} and $\delta^{18}O_{lw}$ values simultaneously, indicating that we may not have captured evaporation correctly. Despite these biases, the model does a good job of replicating modern lake conditions. We further assessed whether our assumptions regarding meteorological inputs for Lake N3 are reasonable using several sensitivity tests of input variables including runoff amount, snowmelt length, and timing, surface incident shortwave radiation, relative humidity and temperature (see supplemental materials, Figure S2).

Next, we ran experiments with the PRYSM lake environment sub-model parameterized for Lake N3 to test the effects of changed seasonal precipitation isotope values and/or amount. These experiments reveal that some scenarios cause Lake N3 water isotope values to change and some do not. $\delta^{18}O_{lw}$ and δ^2H_{lw} follow similar patterns, so δ^2H is discussed in detail throughout this section. In the modern scenario, mean δ^2H_{lw} in Lake N3 ranges from −96.7‰ to −88.5‰ between late fall and winter and the snowmelt, respectively (Figure 3a). Snowmelt, on average, occurs in early June for these experiments. Increased precipitation amount in either the ice-free season (June, July, August, September) or the ice-cover season (October, November, December, January, February) causes lake water to be 8‰ ^{2}H-depleted compared to modern during the ice-cover season. During snowmelt runoff into the lake, increased ice-cover season precipitation amount causes a larger ^{2}H-depletion, 10‰, than increased ice-free season precipitation amount, 5‰, in δ^2H_{lw} values. This change falls within the range of values for the 36 years of model runs of the modern scenario, indicating that precipitation amount alone does not strongly influence Lake N3 water isotope values. ^{2}H-enriched ice-free season precipitation isotopes cause no change in δ^2H_{lw} values. ^{2}H-depleted ice-cover season precipitation isotopes cause δ^2H_{lw} to be about 15‰ and 13‰ ^{2}H-depleted during ice-cover season and snowmelt, respectively, compared to the modern δ^2H_{lw} values. A combination of all scenarios (increased precipitation amount in ice-free season and ice-cover season and ^{2}H-enriched ice-free season and ^{2}H-depleted ice-cover season precipitation isotopes) causes a 16‰ ^{2}H-depletion in ice-cover season and a 21‰ ^{2}H-depletion during the snowmelt relative to the modern δ^2H_{lw} mean. The same scenario but with a higher proportion of precipitation becoming runoff (50% instead of 20%) causes ice-cover season and snow-

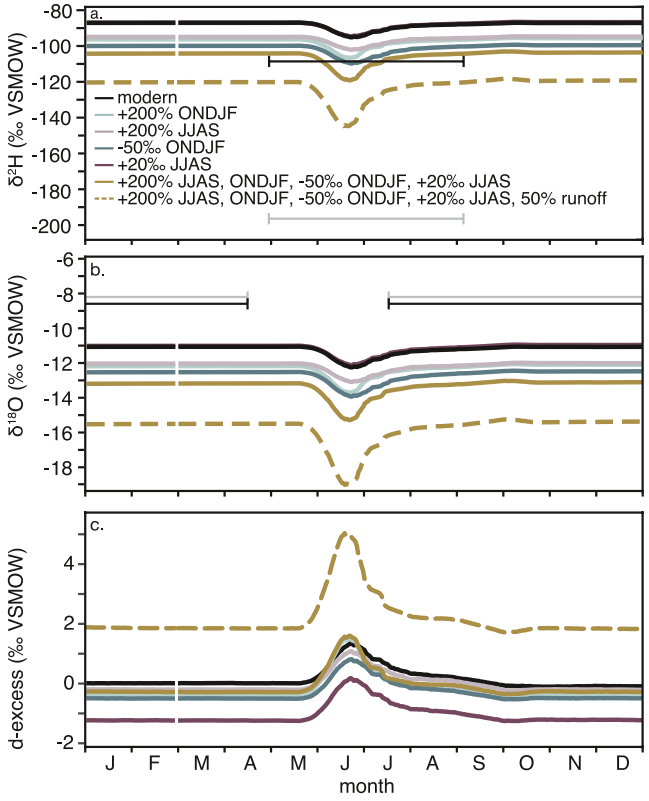

Figure 4. Mean of 36 model years for surface (0–1 m) water isotope values for Lake N3 throughout the year. (a) δ^2H, (b) $\delta^{18}O$, (c) deuterium-excess. Black line used modern parameters. Light purple and light teal were run using 200% increase in ice-free season (JJAS, June, July, August, Septmeber) and ice-cover season (ONDJF, October, November, December, January, February) precipitation, respectively. Dark purple and dark teal were run using 20‰ ^2H-enrichment in JJAS precipitation and 50‰ ^2H-depletion in ONDJF precipitation, respectively. Yellow line is a combination of all four scenarios (increased JJAS, ONDJF, and modified isotopic composition). Solid lines indicate 20% of precipitation was used as runoff, dashed lines indicate 50% of precipitation was used as runoff. Dark purple line is behind black line in panels (a) and (b). All lines are means of 36 years of PRYSM simulation. Black horizontal bar indicates modern lake water δ^2H and $\delta^{18}O$ determined from uppermost sediment sample from C_{24} *n*-alkanoic acid δ^2H and chironomid $\delta^{18}O$ records, plotted during the season when the proxy is produced. Gray horizontal bar indicates the same as black horizontal bar, but for middle Holocene (4–6 ka) lake water δ^2H and $\delta^{18}O$.

melt-season lake surface water to be 20‰ and 34‰ ^2H-depleted compared to modern modeled lake surface water, respectively.

4. Discussion

Lake N3 aquatic plant δ^2H_{wax} and $\delta^{18}O_{chir}$ demonstrate contrasting trends in the mid-Holocene: $\delta^{18}O_{chir}$ becomes ^{18}O-enriched when aquatic δ^2H_{wax} becomes ^2H-depleted, a surprising finding since both proxies form in the same water body (Figure 2). When the chironomid and aquatic plant leaf wax isotope records are converted onto the same δ^2H scale using the local meteoric water line at Lake N3 (Bowen, 2020; Bowen & Revenaugh, 2003; IAEA/WMO, 2020), Lake N3 water δ^2H inferred from chironomids is consistently ^2H-enriched compared to Lake N3 water δ^2H reconstructed from aquatic plant leaf waxes. We interpret these records as reflecting contrasting changes in precipitation seasonality recorded by aquatic δ^2H_{wax} and $\delta^{18}O_{chir}$ at Lake N3, and as reflecting changes in proxy-specific mechanisms throughout the Holocene.

4.1. Interpreting Chironomid $\delta^{18}O$

We examine two possible interpretations of the $\delta^{18}O_{chir}$ record at Lake N3: climatic mechanisms including increases in precipitation amount and precipitation seasonality, or proxy-specific mechanisms. Chironomid larvae in Arctic lakes transition from the third to the fourth instar sometime between late July and the following winter, prior to the spring snow melt (Butler, 1982; Butler & Braegelman, 2018; Lindegaard & Mæhl, 1992; Valero-Garcés et al., 1997). This suggests that because we primarily targeted fourth instar head capsules for this record (all head capsules were in the >125 μm fraction) (Ford, 1959), the $\delta^{18}O_{chir}$ at Lake N3 likely reflects late summer $\delta^{18}O_{lw}$ (Figure 1f), which in turn reflects summer-biased mean annual precipitation $\delta^{18}O$. Climatic factors such as an increase in the amount of summer precipitation during this time would reduce the Lake N3 water residence time during the ice-free season. This means that the ^{18}O-depleted winter precipitation signal would be flushed out of the lake more quickly, causing the lake water to become ^{18}O-enriched, while also reducing the impact of evaporation, which would cause lake water to be ^{18}O-depleted relative to today. PRYSM sensitivity test results (see Section 3.1; Figure 4b) suggest that the lake becomes ^{18}O-depleted when summer precipitation amount increases, suggesting that the decrease in the effect of evaporation dominates the lake water isotope signal for this scenario. Thus, increased summer precipitation amount likely does not explain the observed middle Holocene increase in $\delta^{18}O_{chir}$. Additionally, higher air and sea water temperatures (Axford et al., 2013; Kobashi et al., 2017; Ouellet-Bernier et al., 2014) during the middle Holocene could have caused higher local condensation temperatures and therefore ^{18}O-enriched summer precipitation relative to today. Assuming that summer temperatures in the middle Holocene were 2 °C warmer and using the average Greenland Holocene temperature — $\delta^{18}O$ relationship of 0.36‰/°C (Kobashi et al., 2017; Thomas et al., 2018), then higher summer temperature would account for 0.72‰ of the 3‰ enrichment observed in the $\delta^{18}O_{chir}$ record in the middle Holocene. PRYSM sensitivity test results (see Section 3.1; Figure 4b), however, indicate that increasing summer precipitation $\delta^{18}O$ even by 2.5‰ does not change $\delta^{18}O_{lw}$, suggesting that higher middle Holocene temperatures resulting in ^{18}O-enriched precipitation may not have played a large role in the ^{18}O-enriched $\delta^{18}O_{chir}$ values observed in the middle Holocene. Warmer summer temperatures may also enhance evaporation and lead to ^{18}O-enriched lake water and therefore ^{18}O-enriched $\delta^{18}O_{chir}$ values,

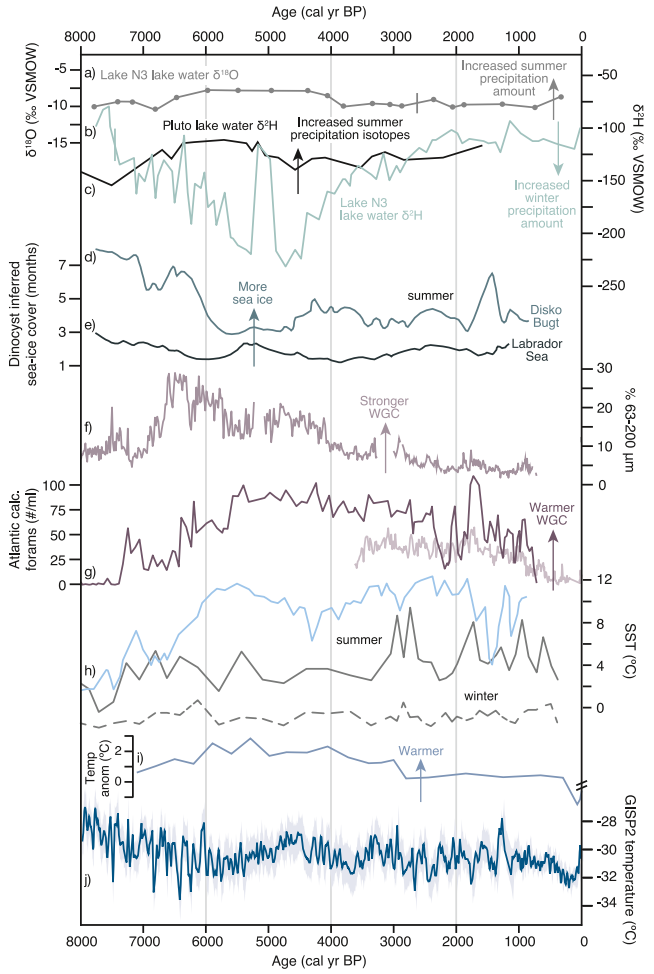

Figure 5. Western Greenland Holocene climate. (a) Fall and winter lake water $\delta^{18}O$ from this study. (b) Spring and summer lake water $\delta^{2}H$ from this study. Vertical lines on (a) and (b) are analytical uncertainty combined with fractionation factor uncertainties. (c) Summer lake water $\delta^{2}H$ inferenced from Pluto Lake C_{20} aquatic plant leaf wax $\delta^{2}H$ (Thomas et al., 2020). (d) and (e) Number of months with 50% or greater sea ice cover in Disko Bugt (MSM334300) and the Labrador Sea (HU84-030-012TWC/PC) inferred from dinocyst assemblages (de Vernal et al., 2013; Ouellet-Bernier et al., 2014). (f) Percent of fine sand in sediment from Disko Bugt, an indicator of the strength of the Western Greenland Current (MSM334310) (Perner et al., 2012). (g) Atlantic calcareous benthic foraminifera concentration from sediment cores in Disko Bugt, indicating Western Greenland Current warmth (MSM334300, MSM334310) (Moros et al., 2016; Perner et al., 2012). (h) Disko Bugt summer sea surface temperature (MSM343300) and Baffin Bay summer and winter (dashed line) sea surface temperature (CC70) inferred from dinocyst assemblages (Gibb et al., 2015; Ouellet-Bernier et al., 2014). (i) Chironomid assemblage-inferred summer air temperature anomaly relative to uppermost sample from North Lake (Axford et al., 2013). (j) Mean annual temperature at GISP2 (Kobashi et al., 2017).

however, PRYSM sensitivity results with increased temperatures and lower relative humidity cause $\delta^{18}O_{lw}$ to become ^{18}O-depleted (Figure S2). Relative humidity, determined from terrestrial and aquatic plant $\delta^{2}H_{wax}$ from Pluto Lake, is higher during the middle Holocene suggesting that there were not significant increases in evaporation during this time (Rach et al., 2017; Thomas et al., 2020). Despite this disagreement between the $\delta^{18}O_{chir}$ record and model results, there may be climatic explanations not captured by our PRYSM sensitivity tests that match the middle Holocene ^{18}O-enriched $\delta^{18}O_{chir}$ record (see Section 4.3).

The Lake N3 $\delta^{18}O_{chir}$ record has trends similar to a record of C_{20} aquatic plant $\delta^{2}H_{wax}$ from Pluto Lake, which shows higher summer $\delta^{2}H_{lw}$ from 7 to 5 ka (Figure 5c). Pluto Lake has a shorter residence time than Lake N3, so aquatic plant leaf waxes produced during the growing season reflect summer precipitation isotopes without a winter bias (Thomas et al., 2020). Therefore, the increase in C_{20} aquatic plant $\delta^{2}H_{wax}$ in Pluto Lake during the Middle Holocene was likely due to ^{2}H-enriched summer precipitation isotopes. The timing of the ^{2}H-enriched values at Pluto Lake is earlier than the ^{18}O-enriched chironomid values at Lake N3. Yet, if both of these records are influenced by the same mechanism, they suggest that summer precipitation on western Greenland may have been enriched in the heavy isotopes during the middle Holocene, perhaps due to a shift to more proximal moisture sources.

4.1.1. Assessing Chironomid-inferred Lake Water $\delta^{18}O$ With Forward Model Results

As discussed above, none of the PRYSM Lake Environment sub-model sensitivity tests of increased precipitation amount or increased precipitation seasonality cause Lake N3 to be ^{18}O-enriched relative to the modern scenario. This suggests that climatic and lake-specific mechanisms likely did not cause the observed middle Holocene $\delta^{18}O_{chir}$ values. Moreover, only two scenarios (longer or later snowmelt), tested while establishing modern conditions of PRYSM for Lake N3 (Figure S2), resulted in late summer lake water values that were ^{18}O-enriched relative to the modern scenario, and those were less than 1‰ enriched, compared to the ~3‰ enrichment in the $\delta^{18}O_{chir}$ record. The rest of the scenarios indicate that $\delta^{18}O_{lw}$ remained constant or became ^{18}O-depleted during the middle Holocene. The measured middle Holocene $\delta^{18}O_{chir}$ is about 6.3‰ ^{18}O-enriched compared to the model scenario where we alter seasonal precipitation isotopes and amount but keep runoff/precipitation ratios constant. Additionally, calculated modern $\delta^{18}O_{chir}$ from modeled modern $\delta^{18}O_{lw}$ using the best-known apparent fractionation factor between and $\delta^{18}O_{chir}$ ($\varepsilon = -22.4 \pm 1.3$‰ (1$\sigma$)), (Figures 4 and S3b.) (Lasher et al., 2017; van Hardenbroek et al., 2018) is about 4.7‰ ^{18}O-depleted compared to the uppermost measured $\delta^{18}O_{chir}$. This disagreement may be partially explained because our uppermost chironomid sample has an age of 328 years BP, and therefore does not reflect modern conditions, but likely does not explain such a large offset. We therefore explore other explanations, including proxy-specific mechanisms, for the differences in the magnitude and direction of the $\delta^{18}O_{chir}$ values and the lake water isotopic response to sensitivity tests in both the modern and middle Holocene.

We used the lake forward model to examine only a limited number of possible climate changes that occurred between the middle and late Holocene. Several other parameters, including the timing and duration of snowmelt, increases in summertime radiation and temperature, and decreases in summertime relative

humidity, also may have changed, causing further modification of the lake water isotope values. Our experiments altering these parameters, while not exhaustive, did not cause the lake water to be as ^{18}O-enriched as the middle Holocene $\delta^{18}O_{chir}$ values (Figure S2), however, changes in chironomid diet may have contributed to the observed middle Holocene ^{18}O-enrichment. About 30% of the oxygen in chironomid head capsules is derived from diet, so changes in diet $\delta^{18}O$ may cause changes in $\delta^{18}O_{chir}$ (Wang et al., 2009). At some sites, however, $\delta^{18}O_{chir}$ mainly records $\delta^{18}O_{lw}$, despite possible changes in diet, which are difficult to constrain through time (Lasher et al., 2017; Wooller et al., 2008). The 3‰ ^{18}O-enrichment in the middle Holocene in the $\delta^{18}O_{chir}$ record is outside of analytical uncertainty, and cannot be explained by changes in $\delta^{18}O_{lw}$ values alone, but may be explained by a combination of minimal changes in $\delta^{18}O_{lw}$ values and slight changes in the chironomid diet. During the middle Holocene, the Lake N3 bulk sediment C:N ratio was about two times higher than the rest of the record, suggesting there may have been an increase in allochthonous terrestrial organic matter to Lake N3 (Figure 2e) (Meyers & Ishiwatari, 1993; Meyers & Lallier-Vergès, 1999). Aquatic macrophytes can also have fairly high C:N ratios (~20–40) in the Arctic, so the increase in the C:N ratio from Lake N3 may due to shifts in the relative amounts of aquatic macrophytes and aquatic algae (Meyers & Ishiwatari, 1993; Vincent et al., 1999). Sauer et al. (2001) examined the $\delta^{18}O$ of lake water and cellulose in lake sediments on Baffin Island and found that disseminated sediment cellulose does not reflect lake water isotopes, but instead is weighted toward terrestrial cellulose values. Whether the increase in the Lake N3 C:N ratio was due to increased amounts of aquatic macrophyte or increased terrestrial organic matter, there would be a concomitant increase in cellulose into the lake sediment (Lasher et al., 2017; Meyers & Lallier-Vergès, 1999). Cellulose can be more than 10‰ ^{18}O-enriched compared to lipids, and $\delta^{18}O$ of terrestrial cellulose can be ^{18}O-enriched relative to aquatic cellulose due to evaporation of source water to terrestrial plants (Sauer et al., 2001; Silva et al., 2015). Either way, an increase in the amount of vascular plant material in the chironomid diet, which is composed of mostly of detritus material and some algae and macrophytes (Henriques-Oliveira et al., 2003), could cause the chironomid head capsules to become ^{18}O-enriched. The Lake N3-specific PRYSM sensitivity tests suggest that proxy-specific mechanisms, in this case diet, may be influencing $\delta^{18}O_{chir}$ in this lake basin more than changes in precipitation seasonality, isotopic composition, or amount. Although the forward model results did match the modern $\delta^{18}O_{lw}$ value, the uppermost $\delta^{18}O_{chir}$ sample did not match modern $\delta^{18}O_{lw}$ value, and the sensitivity tests, which encompass precipitation amount and isotopic changes that could be explained by warmer conditions and more proximal moisture sources, show an opposite direction of change to the $\delta^{18}O_{chir}$ record. These differences may be due to changes in chironomid diet, however, future work to further develop a forward model for the chironomid proxy sensor will help determine the mechanisms causing the isotope shifts observed in the middle Holocene and may improve quantitative estimates of precipitation amount and seasonality.

4.2. Interpreting Aquatic Plant Leaf Wax δ^2H

Lake N3 aquatic plant δ^2H_{wax} becomes ^{2}H-depleted in the middle Holocene, opposite to the Lake N3 $\delta^{18}O_{chir}$ record. Here, we explore both the climatic and proxy-specific mechanisms that may explain this pattern in the aquatic plant waxes. Aquatic plant waxes, in contrast to chironomid head capsules, are produced throughout the ice-free season (Riis et al., 2014), which starts in May at Lake N3 (Thomas et al., 2020). The primary aquatic plant in Lake N3 are aquatic mosses that grow most rapidly throughout the ice-free season (Guo et al., 2013; Thomas et al., 2016), and the chain length distribution of the sedimentary *n*-alkanoic acids is similar to that of modern aquatic mosses (Thomas et al., 2020). We therefore interpret aquatic plant δ^2H_{wax} (here, the C_{24} *n*-alkanoic acid) in Lake N3 to mainly reflect the isotopic composition of lake water during the ice-free season. Today, δ^2H values of Lake N3 water decrease slightly during snowmelt, when ^{2}H-depleted winter precipitation is flushed through Lake N3, and increase throughout summer, due to ^{2}H-enriched summer precipitation and evaporative enrichment of the lake water (Figure 3, S1). Based on the lake water seasonal trajectories and the seasonal production of aquatic plant waxes, possible climatic mechanisms for the observed ^{2}H-depletion of aquatic plant waxes during the middle Holocene include an increase in winter precipitation amount, ^{2}H-depleted winter precipitation relative to the modern, a decrease in the residence time of Lake N3, a decrease in the evaporative enrichment of Lake N3, and earlier lake ice melt causing a decrease in snowmelt bypass (see Thomas et al., 2020 for more details). We use results from the forward

model to assess the above hypotheses about the causes of changes in Lake N3 aquatic δ^2H_{wax} throughout the Holocene. Model results do show ^{2}H-depleted δ^2H_{lw} during several scenarios.

4.2.1. Assessing Leaf Wax-Inferred Lake Water δ^2H With Forward Model Results

In order to compare the measured aquatic δ^2H_{wax} values with the modeled lake water result, we used the best-known apparent fractionation factors between δ^2H_{lw} and C_{24} *n*-alkanoic acid δ^2H, $\varepsilon = -112 \pm 33‰$ (1σ), and calculated δ^2H_{wax} from the modeled lake water using Equation 1 (Figure S3) (McFarlin et al., 2019). δ^2H_{wax} was calculated for the ice-free season, when aquatic plants grow and use lake water to produce waxes, using mean δ^2H_{lw} for that season. Modern δ^2H_{wax} calculated using the modern modeled δ^2H_{lw} is about −196‰ and the measured modern δ^2H_{wax} from sediment is −208‰ (Figure S3). Results from the middle Holocene do not agree in magnitude, however unlike the $\delta^{18}O_{chir}$ record, the shift is in the correct direction. Specifically, in the scenario where both winter and summer precipitation isotopes and amount were changed with 20% precipitation as runoff, lake water during spring was 21‰ depleted compared to the modern. However, this magnitude of change in the model is much less than the magnitude of aquatic δ^2H_{wax} in the middle Holocene, which is more than 100‰ ^{2}H-depleted (Figure 2g). Possible reasons for this disagreement in magnitude of the ^{2}H-depletion of leaf wax in mid Holocene between the measured and modeled results are discussed in detail below.

It is possible that we have not fully constrained the middle Holocene environmental conditions in these PRYSM scenarios, as discussed in in Section 4.1.1. Additionally, runoff amount into Lake N3 both today and during the middle Holocene are difficult to constrain, but may have large impacts on lake water isotope values. For example, if the runoff-to-precipitation ratio were to increase, the lake would be flushed more rapidly during both the spring melt and summer, causing lake water to be ^{2}H-depleted in the growing season, but return to summer precipitation isotope values by the end of the ice-free season (Figure S2). In the sensitivity scenario where we change seasonal precipitation amount and isotopes and increase the amount of precipitation that becomes runoff to 50%, the modeled δ^2H_{wax} value is −155‰, only ~40‰ higher than measured middle Holocene values (Figure 3). An earlier snowmelt due to higher spring temperatures would cause ^{2}H-depleted runoff into the lake earlier in the season, possibly causing a larger amplitude δ^2H_{lw} shift than we have in the PRYSM model results. In contrast, warmer summers may cause the fraction of precipitation that becomes runoff to decrease because a thicker active layer can store more precipitation in soils (Lamhonwah et al., 2017; K. L. Young et al., 1997). It is also possible that the fraction of precipitation that became runoff changed throughout the Holocene after the Greenland Ice Sheet retreated and soils, wetlands, and plant communities developed on the landscape (Michaelson et al., 1998). Quantifying this change is difficult, because we have limited information on the structure of plant communities through the Holocene (Bennike, 2000; Fréchette et al., 2008). In addition, there is little information on how plant communities and soils in the Arctic influence runoff into small lake catchments (K. L. Young et al., 1997). Further investigation of Arctic lake catchment hydrology will improve lake water isotope proxy interpretations. Overall, the PRYSM lake environment sub-model successfully captures modern δ^2H_{lw}, but not the magnitude of change that the aquatic plant waxes record during the middle Holocene. Even so, the sensitivity tests support previous interpretations that at least a portion of the middle Holocene ^{2}H-depletion of Lake N3 water is due to an increase in winter precipitation and a ^{2}H-depletion of winter precipitation caused by sea ice retreat (Thomas et al., 2016, 2020). We explore other possible explanations that may explain why the model does not capture the correct magnitude of change during the middle Holocene.

Similar to the chironomids, there are proxy-specific mechanisms that may influence the aquatic δ^2H_{wax} beyond the climatic explanations discussed above. Different plant species can have different biosynthetic fractionations (Berke et al., 2019; Daniels et al., 2017; Thomas et al., 2020). If the relative amounts of different types of plants species change in a community, then the apparent fractionation between leaf waxes and lake water may shift, which could cause a change in aquatic δ^2H_{wax} without a change in δ^2H_{lw}. Plant community shifts can be constrained by future work that examines past plant community changes via pollen, macrofossils, or sedimentary ancient DNA (Crump et al., 2019; Fréchette & de Vernal, 2009; Thomas et al., 2020). However, the magnitude of change observed in the Lake N3 aquatic plant δ^2H_{wax} is over 100‰, meaning that biosynthetic fractionation values between plant species would need to vary on a similar magnitude, much larger than the differences between modern Arctic plant species (Daniels et al., 2017). We would also expect to see a change in chain length distributions through time if plant species were changing, but we see

no change (with the exception of the oldest three samples), so it is not likely there was a major middle Holocene shift in plant community (Thomas et al., 2020). Despite lack of evidence for plant community changes, our model sensitivity tests did not capture the large-magnitude Middle Holocene changes suggesting that proxy-specific mechanisms may have contributed to the shifts observed in the Lake N3 aquatic δ^2H_{wax} record. Constraining biosynthetic fractionation, especially by aquatic plant species, and plant community shifts through time, will help guide interpretation of this and future records.

4.2.2. Limitations of This Study

There are some assumptions and uncertainties inherent in paleo-water isotope studies such as this one. Analytical uncertainty is 3.0‰ for δ^2H_{wax} (Thomas et al., 2016) and 0.4‰ for $\delta^{18}O_{chir}$. Uncertainties become larger, 33.1‰ and 1.4‰, when δ^2H_{wax} and $\delta^{18}O_{chir}$ are converted to δ^2H_{lw} and $\delta^{18}O_{lw}$, due to large uncertainties in fractionation factors. The fractionation factor determined from Lasher et al. (2017) from chironomids in lake sediment on northwestern Greenland is likely a good representation of the chironomid samples from Lake N3. There are only a few studies of aquatic plant fractionation factors, and we use a global compilation of C_{24} δ^2H_{wax} and δ^2H_{lw}, which does not account for changes in growing season isotopic composition (Aichner et al., 2017; McFarlin et al., 2019).

Furthermore, C_{24} *n*-alkanoic acids are also produced by terrestrial plants, and dominate the C_{24} *n*-alkanoic acid input to some lakes (Dion-Kirschner et al., 2020; McFarlin et al., 2019). However, at Lake N3 the mid-chain (C_{24}) and long-chain (C_{26} and C_{28}) leaf waxes show very different isotopic trends, suggesting that they are from two different plant sources that use two different and very distinct water pools, that is, lake and soil water (Thomas et al., 2016, 2020). Additionally, as indicated in Section 2.5, there are limitations of using PSYRM 2.0 when there is only one set of modern observations from Lake N3 (Figures S4 and S5).

4.3. Holocene Precipitation Amount and Seasonality on Western Greenland

Other Arctic paleoclimate records can be used to assess whether the suggested climatic mechanisms for the middle Holocene changes observed in these western Greenland $\delta^{18}O_{chir}$ and aquatic plant δ^2H_{wax} records may have occurred. Thomas et al., (2016) hypothesized that an increase in winter snowfall was caused by decreased sea ice and warmer surface conditions in Disko Bugt and the Labrador Sea (Figures 5d and 5e) (de Vernal et al., 2013; Ouellet-Bernier et al., 2014). The warmer and stronger western Greenland current (WGC) between 6.5 and 4 ka would have caused greater heat transport to Baffin Bay and Disko Bugt (Figures 1g, 5f, and 5g) (Moros et al., 2016; Perner et al., 2012), causing greater local evaporation, and attendant increases in precipitation amount throughout the year. This hypothesis is supported by a sea surface temperature (SST) reconstruction from Disko Bugt, which shows higher summer SST between 7 and 6 ka (Figure 5h) (Gibb et al., 2015; Ouellet-Bernier et al., 2014). Terrestrial summer air temperature was also higher in the middle Holocene (Figures 5i and 5j) (Axford et al., 2013; Kobashi et al., 2017). Warmer air can hold more moisture, suggesting that there could have been increased evaporation and therefore precipitation amount during the middle Holocene. In addition, higher condensation temperatures would have caused more isotopically enriched summer precipitation during this time. It is possible that increased temperatures during middle Holocene summers may have caused a longer ice-free season, which would have resulted in an earlier snowmelt and more time for evaporation, in turn causing late summer Lake N3 water to be more enriched than today. A decrease in summer precipitation would have had a similar effect: less precipitation would have caused the lake to completely flush slower than today, allowing for greater evaporation. Early summer lake water isotope values (i.e., leaf wax isotopic composition), which are strongly influenced by snowmelt amount, timing, and duration, would have been less impacted than late summer lake water isotope values (i.e., chironomid isotopic composition). We did not test a decreased summer precipitation amount or an earlier snowmelt timing using PRYSM, but future work testing these hypotheses may explain why the $\delta^{18}O_{chir}$ and aquatic plant δ^2H_{wax} records have contrasting trends. Overall, other Arctic records of temperature and WGC strength suggest that there was an increase in precipitation seasonality paired with changes in precipitation amount during the middle Holocene, which may explain some of the changes observed in the $\delta^{18}O_{chir}$ and aquatic plant δ^2H_{wax} records. Further work incorporating a larger range of climate and proxy-specific mechanisms into PRYSM sensitivity tests in the context of these records may

provide a more accurate interpretation of which climate changes and proxy-specific mechanisms explain the observed Holocene trends.

4.4. Implications for Future Paleoclimate Studies

This approach using paired $\delta^{18}O$ and $\delta^{2}H$ records from different proxies in the same sediment archive can be applied in other paleoclimate studies to determine changes in precipitation amount and precipitation isotopes in both winter and summer, provided the study site meets the following guidelines:

4.4.1. Lake Properties

(1) Through-flowing lakes with minimal evaporation reflect precipitation isotopes and are less affected by ^{18}O- and ^{2}H-enrichment that modifies precipitation isotope signals.
(2) Lakes that have a residence time of longer than a month are the best targets for reconstructing precipitation seasonality. The ^{2}H-depleted winter precipitation signal is flushed too quickly from lakes with residence times less than a month, meaning that $\delta^{2}H_{wax}$ does not capture the ^{2}H-depleted winter signal, and will likely not reflect a different seasonal signal than $\delta^{18}O_{chir}$.
(3) Regions with a strong seasonal cycle of precipitation isotopes are ideal candidates for this method. Precipitation that varies seasonally will be reflected in the lake water isotopic composition and will therefore be differentially preserved in the different proxies.
(4) Lakes that are ice-covered for part of the year and are then rapidly flushed by melting winter snowfall during the early summer will likely exhibit strong seasonal signals.

4.4.2. Biotic Properties

(5) Measurable amount of short- or mid-chain waxes sourced from aquatic plants.
(6) In addition, a large quantity of chironomid head capsules is needed in order to make a measurement of $\delta^{18}O$ that is not affected by limited sample size (Wang et al., 2008).
(7) Constraints on chironomid diet and plant community composition through time, and constraints on production seasonality of both proxies, which can influence the isotopic composition of chironomid chitin and aquatic plant leaf waxes.

Chironomids and aquatic plants are found globally, making this dual isotope approach a promising means of reconstructing precipitation seasonality in regions with seasonally varying precipitation isotopes. However, there is evidence that chironomid life cycles are shorter in warmer regions, with some species having multivoltine life cycles (Benbow et al., 2003; Tokeshi, 1995). The isotopic signal would reflect precipitation isotopes throughout the entire growing season if multiple generations of chironomids live and synthesize their head capsules during one summer. Thus, Arctic regions may be the most ideal for reconstructing the seasonally contrasting signals in these two proxies. Regions and lake systems that meet the above parameters are ideal candidates for reconstructing precipitation seasonality using a paired $\delta^{18}O_{chir}$ and $\delta^{2}H_{wax}$ approach. Employing other pairs of proxies may be useful, as well, but obtaining constraints on production seasonality is key.

5. Conclusion

Two lake water isotope proxies from the same lake and sediment samples on western Greenland yield very different patterns through the Holocene. We hypothesize that these two different trends are due to a combination of changes in climate and proxy-specific mechanisms. The two different isotope proxies have distinct seasonal production within the same lake, meaning that $\delta^{18}O_{chir}$ records summer-biased precipitation isotopes and aquatic plant $\delta^{2}H_{wax}$ records winter-biased precipitation isotopes. These two seasonally contrasting proxies therefore may provide an opportunity to reconstruct changes in precipitation amount and isotopic composition during different seasons. Sensitivity tests of the PRYSM Lake Environment sub-model support the hypothesis based on the pair of isotope records that the middle Holocene on western Greenland was wetter during both summer and winter, likely accompanied by an amplified seasonal precipitation isotope signal linked to changes in moisture source. The PRYSM model could not capture the lake system

at Lake N3 completely, highlighting the importance of understanding other lake-specific environmental parameters (e.g., ice melt timing and duration, runoff) and proxy specific-mechanisms (e.g., changes in chironomid diet or in plant community) when interpreting climate records from lake water isotope proxies. Overall, this dual-isotope and lake water modeling approach has the potential to be applied to lakes with similar residence times and in similar geographic settings to infer past changes in precipitation isotopes, amount, and seasonality.

Data Availability Statement

Lake N3 $\delta^{18}O_{chir}$ and leaf wax $\delta^{2}H$ data are freely available online at https://www.ncdc.noaa.gov/paleo/study/20126. Lake model input variables for Lake N3 are available in the Supplement and online at https://doi.org/10.6084/m9.figshare.13713628.

Acknowledgments
The authors would like the thank Joy Matthews for running the chironomid $\delta^{18}O$ samples at UC Davis and to Jason Briner for the sediment samples. This research was supported by NSF grants ARCSS-1504267 and EAR-IF-1652274 to EKT, a Geological Society of America Graduate research grant to MCC, and a Mark Diamond Research Fund grant, funded by the Graduate Student Association at the University at Buffalo, the State University of New York, to MCC.

References

Aichner, B., Hilt, S., Périllon, C., Gillefalk, M., & Sachse, D. (2017). Biosynthetic hydrogen isotopic fractionation factors during lipid synthesis in submerged aquatic macrophytes: Effect of groundwater discharge and salinity. *Organic Geochemistry*, *113*, 10–16. https://doi.org/10.1016/j.orggeochem.2017.07.021

Anderson, L., Abbott, M. B., & Finney, B. P. (2001). Holocene climate inferred from oxygen isotope ratios in lake sediments, central Brooks Range, Alaska. *Quaternary Research*, *55*(3), 313–321. https://doi-org.proxy.libraries.uc.edu/10.1006/qres.2001.2219

Anderson, N. J., & Leng, M. J. (2004). Increased aridity during the early Holocene in West Greenland inferred from stable isotopes in laminated-lake sediments. *Quaternary Science Reviews*, *23*(7), 841–849. https://doi.org/10.1016/j.quascirev.2003.06.013

Andreev, A. A., & Klimanov, V. A. (2000). Quantitative Holocene climatic reconstruction from Arctic Russia. *Journal of Paleolimnology*, *24*(1), 81–91. https://doi.org/10.1023/A:1008121917521

Andresen, C. S., Björck, S., Bennike, O., & Bond, G. (2004). Holocene climate changes in southern Greenland: Evidence from lake sediments. *Journal of Quaternary Science*, *19*(8), 783–795. https://doi-org.proxy.libraries.uc.edu/10.1002/jqs.886

Arppe, L., Kurki, E., Wooller, M. J., Luoto, T. P., Zajączkowski, M., & Ojala, A. E. (2017). A 5500-year oxygen isotope record of high arctic environmental change from southern Spitsbergen. *The Holocene*, *27*(12), 1948–1962. https://doi.org/10.1177/0959683617715698

Axford, Y., Losee, S., Briner, J. P., Francis, D. R., Langdon, P. G., & Walker, I. R. (2013). Holocene temperature history at the western Greenland ice sheet margin reconstructed from lake sediments. *Quaternary Science Reviews*, *59*, 87–100. https://doi.org/10.1016/j.quascirev.2012.10.024

Balascio, N. L., D'Andrea, W. J., Bradley, R. S., & Perren, B. B. (2013). Biogeochemical evidence for hydrologic changes during the Holocene in a lake sediment record from southeast Greenland. *The Holocene*, *23*(10), 1428–1439. https://doi.org/10.1177/0959683613493938

Balascio, N. L., D'Andrea, W. J., Gjerde, M., & Bakke, J. (2018). Hydroclimate variability of high Arctic Svalbard during the Holocene inferred from hydrogen isotopes of leaf waxes. *Quaternary Science Reviews*, *183*(10), 177–187. http://dx.doi.org/10.1016/j.quascirev.2016.11.036

Benbow, M. E., Burky, A. J., & Way, C. M. (2003). Life cycle of a torrenticolous Hawaiian chironomid (Telmatogeton torrenticola) : Stream flow and microhabitat effects. *Annales de Limnologie - International Journal of Limnology*, *39*(2), 103–114. https://doi.org/10.1051/limn/2003008

Bennike, O. (2000). Palaeoecological studies of Holocene lake sediments from west Greenland. *Palaeogeography, Palaeoclimatology, Palaeoecology*, *155*(3), 285–304. https://doi.org/10.1016/S0031-0182(99)00121-2

Berke, M. A., Cartagena Sierra, A., Bush, R., Cheah, D., & O'Connor, K. (2019). Controls on leaf wax fractionation and $\delta^{2}H$ values in tundra vascular plants from western Greenland. *Geochimica et Cosmochimica Acta*, *244*, 565–583. https://doi.org/10.1016/j.gca.2018.10.020

Bintanja, R., & Selten, F. M. (2014). Future increases in Arctic precipitation linked to local evaporation and sea-ice retreat. *Nature*, *509*(7501), 479–482. https://doi.org/10.1038/nature13259

Bowen, G. J. (2020). *The online isotopes in precipitation calculator, version 3.1*. The University of Utah. Accessible at http://www.waterisotopes.org

Bowen, G. J., Cai, Z., Fiorella, R. P., & Putman, A. L. (2019). Isotopes in the water cycle: Regional to global-scale patterns and applications. *Annual Review of Earth and Planetary Sciences*, *47*(1), 453–479. https://doi.org/10.1146/annurev-earth-053018-060220

Bowen, G. J., Chesson, L., Nielson, K., Cerling, T. E., & Ehleringer, J. R. (2005). Treatment methods for the determination of δ2H and δ18O of hair keratin by continuous-flow isotope-ratio mass spectrometry. *Rapid Communications in Mass Spectrometry*, *19*(17), 2371–2378. https://doi.org/10.1002/rcm.2069

Bowen, G. J., & Revenaugh, J. (2003). Interpolating the isotopic composition of modern meteoric precipitation. *Water Resources Research*, *39*(10). 1299. https://doi.org/10.1029/2003WR002086

Briner, J. P., Stewart, H. A. M., Young, N. E., Philipps, W., & Losee, S. (2010). Using proglacial-threshold lakes to constrain fluctuations of the Jakobshavn Isbræ ice margin, western Greenland, during the Holocene. *Quaternary Science Reviews*, *29*(27), 3861–3874. https://doi.org/10.1016/j.quascirev.2010.09.005

Butler, M. G. (1982). A 7-year life cycle for two Chironomus species in Arctic Alaskan tundra ponds (Diptera: Chironomidae). *Canadian Journal of Zoology*, *60*(1), 58–70. https://doi.org/10.1139/z82-008

Butler, M. G., & Braegelman, S. D. (2018). Pre-emergence growth and development in the Arctic midge Trichotanypus alaskensis Brundin: Pre-emergence growth and development in Trichotanypus alaskensis. *Journal of Limnology*, *77*(1). https://doi.org/10.4081/jlimnol.2018.1836

Castañeda, I. S., & Schouten, S. (2011). A review of molecular organic proxies for examining modern and ancient lacustrine environments. *Quaternary Science Reviews*, *30*(21–22), 2851–2891. https://doi.org/10.1016/j.quascirev.2011.07.009

Cluett, A. A., & Thomas, E. K. (2020). Resolving combined influences of inflow and evaporation on western Greenland lake water isotopes to inform paleoclimate inferences. *Journal of Paleolimnology*, *63*, 251–268. https://doi.org/10.1007/s10933-020-00114-4

Corcoran, M. C., Diefendorf, A. F., Lowell, T. V., Freimuth, E. J., Schartman, A. K., Bates, B. R., et al. (2020). Hydrogen isotopic composition (δ2H) of diatom-derived C20 highly branched isoprenoids from lake sediments track lake water δ2H. *Organic Geochemistry*, *150*, 104122. http://www.sciencedirect.com/science/article/pii/S0146638020301571

Crump, S. E., Miller, G. H., Power, M., Sepúlveda, J., Dildar, N., Coghlan, M., & Bunce, M. (2019). Arctic shrub colonization lagged peak postglacial warmth: Molecular evidence in lake sediment from Arctic Canada. *Global Change Biology*, *25*(12), 4244–4256. https://doi.org/10.1111/gcb.14836

Cuffey, K. M., & Clow, G. D. (1997). Temperature, accumulation, and ice sheet elevation in central Greenland through the last deglacial transition. *Journal of Geophysical Research*, *102*(C12), 26383–26396. https://doi.org/10.1029/96JC03981

Cuffey, K. M., & Steig, E. J. (1998). Isotopic diffusion in polar firn: Implications for interpretation of seasonal climate parameters in ice-core records, with emphasis on central Greenland. *Journal of Glaciology*, *44*(147), 273–284. https://doi.org/10.3189/S0022143000002616

Daniels, W. C., Russell, J. M., Giblin, A. E., Welker, J. M., Klein, E. S., & Huang, Y. (2017). Hydrogen isotope fractionation in leaf waxes in the Alaskan Arctic tundra. *Geochimica et Cosmochimica Acta*, *213*, 216–236. https://doi.org/10.1016/j.gca.2017.06.028

Dansgaard, W. (1964). Stable isotopes in precipitation. *Tellus*, *16*(4), 436–468

Dee, S. G., Emile-Geay, J., Evans, M. N., Allam, A., Steig, E. J., & Thompson, D. M. (2015). PRYSM: An open-source framework for PRoxY system modeling, with applications to oxygen-isotope systems. *Journal of Advances in Modeling Earth Systems*, *7*, 1220–1247. https://doi.org/10.1002/2015MS000447

Dee, S. G., Russell, J. M., Morrill, C., Chen, Z., & Neary, A. (2018). PRYSM v2.0: A proxy system model for lacustrine archives. *Paleoceanography and Paleoclimatology*, *33*, 1250–1269. https://doi.org/10.1029/2018PA003413

de Vernal, A., Hillaire-Marcel, C., Rochon, A., Fréchette, B., Henry, M., Solignac, S., & Bonnet, S. (2013). Dinocyst-based reconstructions of sea ice cover concentration during the Holocene in the Arctic Ocean, the northern North Atlantic Ocean and its adjacent seas. *Quaternary Science Reviews*, *79*, 111–121. https://doi.org/10.1016/j.quascirev.2013.07.006

Dion-Kirschner, H., McFarlin, J. M., Masterson, A. L., Axford, Y., & Osburn, M. R. (2020). Modern constraints on the sources and climate signals recorded by sedimentary plant waxes in west Greenland. *Geochimica et Cosmochimica Acta*, *286*, 336–354. https://doi.org/10.1016/j.gca.2020.07.027

FitzGibbon, J., & Dunne, T. (1981). Land surface and lake storage during snowmelt runoff in a subarctic drainage system. *Arctic and Alpine Research*, *13*(3), 277–285. https://doi.org/10.2307/1551034

Ford, J. B. (1959). A study of larval growth, the number of instars and sexual differentiation in the Chironomidae (Diptera). *Proceedings of the Royal Entomological Society of London. Series A, General Entomology*, *34*(10-12), 151–160. https://doi.org/10.1111/j.1365-3032.1959.tb00231.x

Fréchette, B., & de Vernal, A. (2009). Relationship between Holocene climate variations over southern Greenland and eastern Baffin Island and synoptic circulation pattern. *Climate of the Past*, *5*(3), 347–359. https://doi.org/10.5194/cp-5-347-2009

Fréchette, B., de Vernal, A., Guiot, J., Wolfe, A. P., Miller, G. H., Fredskild, B., et al. (2008). Methodological basis for quantitative reconstruction of air temperature and sunshine from pollen assemblages in Arctic Canada and Greenland. *Quaternary Science Reviews*, *27*(11), 1197–1216. https://doi.org/10.1016/j.quascirev.2008.02.016

Gibb, O. T., Steinhauer, S., Fréchette, B., de Vernal, A., & Hillaire-Marcel, C. (2015). Diachronous evolution of sea surface conditions in the Labrador Sea and Baffin Bay since the last deglaciation. *The Holocene*, *25*(12), 1882–1897. https://doi.org/10.1177/0959683615591352

Gibson, J. J. (2002). Short-term evaporation and water budget comparisons in shallow Arctic lakes using non-steady isotope mass balance. *Journal of Hydrology*, *264*(1), 242–261. https://doi.org/10.1016/S0022-1694(02)00091-4

Gibson, J. J., Birks, S. J., & Yi, Y. (2016). Stable isotope mass balance of lakes: A contemporary perspective. *Quaternary Science Reviews*, *131*(Part B), 316–328. https://doi.org/10.1016/j.quascirev.2015.04.013

Gibson, J. J., Prepas, E. E., & McEachern, P. (2002). Quantitative comparison of lake throughflow, residency, and catchment runoff using stable isotopes: Modeling and results from a regional survey of Boreal lakes. *Journal of Hydrology*, *262*(1–4), 128–144. https://doi.org/10.1016/S0022-1694(02)00022-7

Guo, C.-Q., Ochyra, R., Wu, P.-C., Seppelt, R. D., Yao, Y.-F., Bian, L.-G., et al. (2013). Warnstorfia exannulata, an aquatic moss in the Arctic: Seasonal growth responses. *Climatic Change*, *119*(2), 407–419. https://doi.org/10.1007/s10584-013-0724-5

Henriques-Oliveira, A. L., Nessimian, J. L., & Dorvillé, L. F. (2003). Feeding habits of chironomid larvae (Insecta: Diptera) from a stream in the Floresta da Tijuca, Rio de Janeiro, Brazil. *Brazilian Journal of Biology*, *63*(2), 269–281. https://doi.org/10.1590/S1519-69842003000200012

Hershey, A. E. (1985). Littoral chironomid communities in an arctic Alaskan lake. *Ecography*, *8*(1), 39–48. https://doi.org/10.1111/j.1600-0587.1985.tb01150.x

Hostetler, S. W., & Bartlein, P. J. (1990). Simulation of lake evaporation with application to modeling lake level variations of Harney-Malheur Lake, Oregon. *Water Resources Research*, *26*(10), 2603–2612. https://doi/abs/10.1029/WR026i010p02603

Hostetler, S. W., & Benson, L. V. (1994). Stable isotopes of oxygen and hydrogen in the Truckee River–Pyramid Lake surface-water system. 2. A predictive model of δ18O and 182H in Pyramid lake. *Limnology and Oceanography*, *39*(2), 356–364. https://doi/abs/10.4319/lo.1994.39.2.0356

IAEA/WMO. (2020). Global network of isotopes in precipitation. *The GNIP Database*. Accessible at https://nucleus.iaea.org/wiser

Jepsen, S., Voss, C., Walvoord, M., Rose, J., Minsley, B., & Smith, B. (2013). Sensitivity analysis of lake mass balance in discontinuous permafrost: The example of disappearing Twelvemile Lake, Yukon Flats, Alaska (USA). *Hydrogeology Journal*. *21*(1), 185–200. https://doi.org/10.1007/s10040-012-0896-5

Jonsson, C. E., Leng, M. J., Rosqvist, G. C., Seibert, J., & Arrowsmith, C. (2009). Stable oxygen and hydrogen isotopes in sub-Arctic lake waters from northern Sweden. *Journal of Hydrology*, *376*(1), 143–151. https://doi.org/10.1016/j.jhydrol.2009.07.021

Kaufman, D. S., Ager, T. A., Anderson, N. J., Anderson, P. M., Andrews, J. T., Bartlein, P. J., et al. (2004). Holocene thermal maximum in the western Arctic (0–180°W). *Quaternary Science Reviews*, *23*(5), 529–560. https://doi.org/10.1016/j.quascirev.2003.09.007

Kobashi, T., Menviel, L., Jeltsch-Thömmes, A., Vinther, B. M., Box, J. E., Muscheler, R., et al. (2017). Volcanic influence on centennial to millennial Holocene Greenland temperature change. *Scientific Reports*, *7*(1), 1–10. https://doi.org/10.1038/s41598-017-01451-7

Kopec, B. G., Feng, X., Michel, F. A., & Posmentier, E. S. (2016). Influence of sea ice on Arctic precipitation. *Proceedings of the National Academy of Sciences*, *113*(1), 46–51. https://doi.org/10.1073/pnas.1504633113

Krabill, W., Hanna, E., Huybrechts, P., Abdalati, W., Cappelen, J., Csatho, B., et al. (2004). Greenland Ice Sheet: Increased coastal thinning. *Geophysical Research Letters*, *31*. https://doi.org/10.1029/2004GL021533

Lamhonwah, D., Lafrenière, M. J., Lamoureux, S. F., & Wolfe, B. B. (2017). Evaluating the hydrological and hydrochemical responses of a High Arctic catchment during an exceptionally warm summer. *Hydrological Processes*, *31*(12), 2296–2313. https://doi.org/10.1002/hyp.11191

Lasher, G. E., Axford, Y., Masterson, A. L., Berman, K., & Larocca, L. J. (2020). Holocene temperature and landscape history of southwest Greenland inferred from isotope and geochemical lake sediment proxies. *Quaternary Science Reviews*, *239*, 106358. https://doi.org/10.1016/j.quascirev.2020.106358

Lasher, G. E., Axford, Y., McFarlin, J. M., Kelly, M. A., Osterberg, E. C., & Berkelhammer, M. B. (2017). Holocene temperatures and isotopes of precipitation in Northwest Greenland recorded in lacustrine organic materials. *Quaternary Science Reviews*, *170*, 45–55. https://doi.org/10.1016/j.quascirev.2017.06.016

Lindegaard, C., & Mæhl, P. (1992). Abundance, population dynamics and production of Chironomidae (Diptera) in an ul traoligotrophic lake in South greenland. *Netherland Journal of Aquatic Ecology*, *26*(2), 297–308. https://doi.org/10.1007/BF02255255

Masson-Delmotte, V., Landais, A., Stievenard, M., Cattani, O., Falourd, S., Jouzel, J., et al. (2005). Holocene climatic changes in Greenland: Different deuterium excess signals at Greenland ice core project (GRIP) and NorthGRIP, *Journal of Geophysical Research*, *110*, D14102. https://doi.org/10.1029/2004JD005575

McFarlin, J. M., Axford, Y., Masterson, A. L., & Osburn, M. R. (2019). Calibration of modern sedimentary δ^2H plant wax-water relationships in Greenland lakes. *Quaternary Science Reviews*, *225*, 105978. https://doi.org/10.1016/j.quascirev.2019.105978

McMillan, M., Leeson, A., Shepherd, A., Briggs, K., Armitage, T. W. K., Hogg, A., et al. (2016). A high-resolution record of Greenland mass balance. *Geophysical Research Letters*, *43*(13), 7002–7010. https://doi.org/10.1002/2016GL069666

Meyers, P. A., & Ishiwatari, R. (1993). Lacustrine organic geochemistry—an overview of indicators of organic matter sources and diagenesis in lake sediments. *Organic Geochemistry*, *20*(7), 867–900. https://doi.org/10.1016/0146-6380(93)90100-

Meyers, P. A., & Lallier-Vergès, E. (1999). Lacustrine sedimentary organic matter records of Late Quaternary paleoclimates. *Journal of Paleolimnology*, *21*(3), 345–372. https://doi.org/10.1023/A:1008073732192

Michaelson, G. J., Ping, C. L., Kling, G. W., & Hobbie, J. E. (1998). The character and bioactivity of dissolved organic matter at thaw and in the spring runoff waters of the arctic tundra North Slope, Alaska. *Journal of Geophysical Research*, *103*(D22), 28939–28946. https://doi.org/10.1029/98JD02650

Moros, M., Lloyd, J. M., Perner, K., Krawczyk, D., Blanz, T., de Vernal, A., et al. (2016). Surface and sub-surface multi-proxy reconstruction of middle to late Holocene palaeoceanographic changes in Disko Bugt, West Greenland. *Quaternary Science Reviews*, *132*, 146–160. https://doi.org/10.1016/j.quascirev.2015.11.017

Morrill, C., Meador, E., Livneh, B., Liefert, D. T., & Shuman, B. N. (2019). Quantitative model-data comparison of mid-Holocene lake-level change in the central Rocky mountains. *Climate Dynamics*, *53*(1), 1077–1094. https://doi.org/10.1007/s00382-019-04633-3

Nerem, R. S., Beckley, B. D., Fasullo, J. T., Hamlington, B. D., Masters, D., & Mitchum, G. T. (2018). Climate-change–driven accelerated sea-level rise detected in the altimeter era. *Proceedings of the National Academy of Sciences*, *115*(9), 2022–2025. https://doi.org/10.1073/pnas.1717312115

Nichols, J. E., Walcott, M., Bradley, R., Pilcher, J., & Huang, Y. (2009). Quantitative assessment of precipitation seasonality and summer surface wetness using ombrotrophic sediments from an Arctic Norwegian peatland. *Quaternary Research*, *72*(3), 443–451. https://doi.org/10.1016/j.yqres.2009.07.007

NOAA. (2020). Global historical climatology network. *National Climatic Data Center (NCDC)*. Accessible at. http://www.ncdc.noaa.gov

Ouellet-Bernier, M.-M., Vernal, A. d., Hillaire-Marcel, C., & Moros, M. (2014). Paleoceanographic changes in the Disko Bugt area, West Greenland, during the Holocene. *The Holocene*, *24*(11), 1573–1583. https://doi.org/10.1177/0959683614544060

Perner, K., Moros, M., Jennings, A., Lloyd, J. M., & Knudsen, K. L. (2012). Holocene palaeoceanographic evolution off West Greenland. *The Holocene*, *23*(3), 374–387. https://doi.org/10.1177/0959683612460785

Post, E., Forchhammer, M. C., Bret-Harte, M. S., Callaghan, T. V., Christensen, T. R., Elberling, B., et al. (2009). Ecological dynamics across the arctic associated with recent climate change. *Science*, *325*(5946), 1355–1358. https://doi.org/10.1126/science.1173113

Rach, O., Kahmen, A., Brauer, A., & Sachse, D. (2017). A dual-biomarker approach for quantification of changes in relative humidity from sedimentary lipid D/H ratios. *Climate of the Past*, *13*(7), 741–757. https://doi.org/10.5194/cp-13-741-2017

Reiter, P., Gutjahr, O., Schefczyk, L., Heinemann, G., & Casper, M. (2018). Does applying quantile mapping to subsamples improve the bias correction of daily precipitation? *International Journal of Climatology*, *38*(4), 1623–1633. https://doi.org/10.1002/joc.5283

Riis, T., Christoffersen, K. S., & Baattrup-Pedersen, A. (2014). Effects of warming on annual production and nutrient-use efficiency of aquatic mosses in a high Arctic lake. *Freshwater Biology*, *59*(8), 1622–1632. https://doi.org/10.1111/fwb.12368

Roulet, N. T., & Woo, M.-K. (1988). Runoff generation in a low Arctic drainage basin. *Journal of Hydrology*, *101*(1), 213–226. https://doi.org/10.1016/0022-1694(88)90036-4

Sachse, D., Billault, I., Bowen, G. J., Chikaraishi, Y., Dawson, T. E., Feakins, S. J., et al. (2012). Molecular paleohydrology: interpreting the hydrogen-isotopic composition of lipid biomarkers from photosynthesizing organisms. *Annual Review of Earth and Planetary Sciences*, *40*(1), 221–249. https://doi.org/10.1146/annurev-earth-042711-105535

Sachse, D., Radke, J., & Gleixner, G. (2006). D values of individual n-alkanes from terrestrial plants along a climatic gradient - Implications for the sedimentary biomarker record. *Organic Geochemistry*, *37*(4), 469–483. https://doi.org/10.1016/j.orggeochem.2005.12.003

Sauer, P. E., Miller, G. H., & Overpeck, J. T. (2001). Oxygen isotope ratios of organic matter in arctic lakes as a paleoclimate proxy: field and laboratory investigations. *Journal of Paleolimnology*, *25*(1), 43–64. https://doi.org/10.1023/A:1008133523139

Saulnier-Talbot, E., Leng, M. J., & Pienitz, R. (2007). Recent climate and stable isotopes in modern surface waters of northernmost Ungava Peninsula, Canada. *Canadian Journal of Earth Sciences*, *44*, 171. Article. https://doi.org/10.1139/e06-089

Schiff, C., Kaufman, D., Wolfe, A., Dodd, J., & Sharp, Z. (2009). Late Holocene storm-trajectory changes inferred from the oxygen isotope composition of lake diatoms, south Alaska. *Journal of Paleolimnology*, *41*(1), 189–208. https://doi.org/10.1007/s10933-008-9261-z

Silva, L. C. R., Pedroso, G., Doane, T. A., Mukome, F. N. D., & Horwath, W. R. (2015). Beyond the cellulose: Oxygen isotope composition of plant lipids as a proxy for terrestrial water balance. *Geochemical Perspectives Letters*, *1*(1), 33–42. https://doi.org/10.7185/geochemlet.1504

Thomas, E. K., Briner, J. P., Ryan-Henry, J. J., & Huang, Y. (2016). A major increase in winter snowfall during the middle Holocene on western Greenland caused by reduced sea ice in Baffin Bay and the Labrador Sea. *Geophysical Research Letters*, *43*(10), 5302–5308. https://doi.org/10.1002/2016GL068513

Thomas, E. K., Castañeda, I. S., McKay, N. P., Briner, J. P., Salacup, J. M., Nguyen, K. Q., & Schweinsberg, A. D. (2018). A wetter Arctic coincident with hemispheric warming 8,000 years ago. *Geophysical Research Letters*, *45*(19), 10637–10647. https://doi.org/10.1029/2018GL079517

Thomas, E. K., Hollister, K. V., Cluett, A. A., & Corcoran, M. C. (2020). Reconstructing arctic precipitation seasonality using aquatic leaf wax δ2h in lakes with contrasting residence times. *Paleoceanography and Paleoclimatology*, *35*, e2020PA003886. https://doi.org/10.1029/2020PA003886

Tipple, B. J., Berke, M. A., Doman, C. E., Khachaturyan, S., & Ehleringer, J. R. (2013). Leaf-wax n-alkanes record the plant–water environment at leaf flush. *Proceedings of the National Academy of Sciences*, *110*(7), 2659–2664. https://doi.org/10.1073/pnas.1213875110

Tokeshi, M. (1995). Life cycles and population dynamics. In *The chironomidae* (pp. 225–268). Springer.

Tondu, J. M. E., Turner, K. W., Wolfe, B. B., Hall, R. I., Edwards, T. W. D., & McDonald, I. (2013). Using water isotope tracers to develop the hydrological component of a long-term aquatic ecosystem monitoring program for a northern lake-rich landscape. *Arctic Antarctic and Alpine Research*, *45*(4), 594–614. https://doi.org/10.1657/1938-4246-45.4.594

Valero-Garcés, B. L., Laird, K. R., Fritz, S. C., Kelts, K., Ito, E., & Grimm, E. C. (1997). Holocene climate in the northern great plains inferred from sediment stratigraphy, stable isotopes, carbonate geochemistry, diatoms, and pollen at Moon Lake, North Dakota. *Quaternary Research*, *48*(3), 359–369. https://doi.org/10.1006/qres.1997.1930

van Hardenbroek, M., Chakraborty, A., Davies, K. L., Harding, P., Heiri, O., Henderson, A. C. G., et al. (2018). The stable isotope composition of organic and inorganic fossils in lake sediment records: Current understanding, challenges, and future directions. *Quaternary Science Reviews*, *196*, 154–176. https://doi.org/10.1016/j.quascirev.2018.08.003

Verbruggen, F., Heiri, O., Reichart, G. J., Blaga, C., & Lotter, A. F. (2011). Stable oxygen isotopes in chironomid and cladoceran remains as indicators for lake-water δ18O. *Limnology and Oceanography*, *56*(6), 2071–2079. https://doi.org/10.4319/lo.2011.56.6.2071

Verbruggen, F., Heiri, O., Reichart, G.-J., De Leeuw, J. W., Nierop, K. G. J., & Lotter, A. F. (2010). Effects of chemical pretreatments on δ18O measurements, chemical composition, and morphology of chironomid head capsules. *Journal of Paleolimnology*, *43*(4), 857–872. https://doi.org/10.1007/s10933-009-9374-z

Vincent, W. F., Riis, T., Markager, S., & Sand-Jensen, K. (1999). Slow growth and decomposition of mosses in Arctic lakes. *Canadian Journal of Fisheries and Aquatic Sciences*, *56*(3), 388–393. https://doi.org/10.1139/f98-184

Wang, Y. V., Francis, D. R., O'Brien, D. M., & Wooller, M. J. (2008). A protocol for preparing subfossil chironomid head capsules (Diptera: Chironomidae) for stable isotope analysis in paleoclimate reconstruction and considerations of contamination sources. *Journal of Paleolimnology*, *40*(3), 771–781. https://doi.org/10.1007/s10933-008-9197-3

Wang, Y. V., O'Brien, D. M., Jenson, J., Francis, D., & Wooller, M. J. (2009). The influence of diet and water on the stable oxygen and hydrogen isotope composition of Chironomidae (Diptera) with paleoecological implications. *Oecologia*, *160*(2), 225–233. https://doi.org/10.1007/s00442-009-1303-3

Welp, L. R., Randerson, J. T., Finlay, J. C., Davydov, S. P., Zimova, G. M., Davydova, A. I., & Zimov, S. A. (2005). A high-resolution time series of oxygen isotopes from the Kolyma River: Implications for the seasonal dynamics of discharge and basin-scale water use. *Geophysical Research Letters*, *32*, L14401. https://doi.org/10.1029/2005GL022857

Wooller, M., Wang, Y., & Axford, Y. (2008). A multiple stable isotope record of Late Quaternary limnological changes and chironomid paleoecology from northeastern Iceland. *Journal of Paleolimnology*, *40*(1), 63–77. https://doi.org/10.1007/s10933-007-9144-8

Young, K. L., Woo, M., & Edlund, S. A. (1997). Influence of local topography, soils, and vegetation on microclimate and hydrology at a high arctic site, Ellesmere Island, Canada. *Arctic and Alpine Research*, *29*(3), 270–284. https://doi.org/10.1080/00040851.1997.12003245

Young, N. E., Briner, J. P., Rood, D. H., Finkel, R. C., Corbett, L. B., & Bierman, P. R. (2013). Age of the Fjord Stade moraines in the Disko Bugt region, western Greenland, and the 9.3 and 8.2 ka cooling events. *Quaternary Science Reviews*, *60*, 76–90. https://doi.org/10.1016/j.quascirev.2012.09.028